BRNO UNIVERSITY OF TECHNOLOGY
VYSOKÉ UČENÍ TECHNICKÉ V BRNĚ

FACULTY OF CHEMISTRY
FAKULTA CHEMICKÁ

INSTITUTE OF PHYSICAL AND APPLIED CHEMISTRY
ÚSTAV FYZIKÁLNÍ A SPOTŘEBNÍ CHEMIE

THE EFFECT OF BIOPOLYMERS ON ADHESIVE AND RHEOLOGICAL PROPERTIES OF CALCIUM PHOSPHATE BONE CEMENTS

VLIV BIOPOLYMERŮ NA ADHEZIVNÍ A REOLOGICKÉ VLASTNOSTI CEMENTŮ Z FOSFOREČNANU VÁPENATÉHO

BACHELOR'S THESIS
BAKALÁŘSKÁ PRÁCE

AUTHOR — **David Scholz**
AUTOR PRÁCE

SUPERVISOR — **doc. Ing. Lucy Vojtová, Ph.D.**
VEDOUCÍ PRÁCE

BRNO 2020

BRNO UNIVERSITY OF TECHNOLOGY
FACULTY OF CHEMISTRY

Specification Bachelor's Thesis

Project no.:	FCH-BAK1538/2019	Academic year:	2019/20
Department:	Institute of Physical and Applied Chemistry		
Student:	**David Scholz**		
Study programme:	Chemistry and Chemical Technologies		
Study branch:	Chemistry for Medical Applications		
Head of thesis:	**doc. Ing. Lucy Vojtová, Ph.D.**		

Title of Bachelor's Thesis:

The effect of biopolymers on adhesive and rheological properties of calcium phosphate bone cements

Bachelor's Thesis:

1) Literary searching on polymeric adhesives for phosphate cements.
2) Preparation of samples of phosphate cements with biopolymers and crosslinking agents.
3) Monitoring of the influence of biopolymers on adhesive, mechanical and rheological properties of cement.
4) Evaluation of results and their discussion.
5) Conclusion.

Deadline for Bachelor's Thesis delivery: 31.7.2020:

Bachelor's Thesis should be submitted to the institute's secretariat in a number of copies as set by the dean This specification is part of Bachelor's Thesis

David Scholz Student	doc. Ing. Lucy Vojtová, Ph.D. Head of thesis	prof. Ing. Miloslav Pekař, CSc. Head of department

In Brno dated 31.1.2020

prof. Ing. Martin Weiter, Ph.D.
Dean

ABSTRACT

This thesis deals with bone cement composed of tricalcium phosphate and thermosensitive copolymer. The main aim was to improve especially the adhesive properties of the cement by adding polysaccharide.

The theoretical part of the thesis deals with the characterization of bone cements and their application and also a description of polymeric additives used in bone cements mainly focused on polysaccharides.

In the experimental part, the prepared cements were characterized using rheology, powder X-ray diffraction and static mechanical tests on the cured cement alone and glued bones. Rheology was used to measure the setting time of the cements as a function of time and temperature. Furthermore, rheology was also intended to measure the adhesive properties of copolymer solutions, but this was not possible due to the nonreproducible results caused by inhomogeneity of the copolymer solutions with polysaccharide. Powder X-ray diffraction was used to measure the effect of polysaccharide on the conversion of tricalcium phosphate to calcium deficient hydroxyapatite. It was found out that polysaccharide does not significantly affect the conversion of tricalcium phosphate. Static mechanical tests were used to measure maximal compressive strength for the cured cement samples and also to measure the adhesion strength of glued bone samples. Cured samples with low polysaccharide concentration showed higher compressive strength compared to control samples. Inconclusive results were obtained during testing of the bone samples due to the complexity of the measurement. In particular, it concerns the preparation of bone samples and their gluing with bone cement.

KEYWORDS

Bone cement, calcium phosphate cement, thermosensitive copolymer, polysaccharide, rheology, adhesion, powder X-ray diffraction, mechanical testing.

ABSTRAKT

Tato práce se zabývá kostním cementem složeného z fosforečnanu vápenatého a termosenzitivního kopolymeru. Hlavním cílem bylo vylepšení zejména adhezivních vlastností cementu přídavkem polysacharidu.

Teoretická část práce se zabývá charakterizací kostních cementů a jejich aplikací. Dále také popisem polymerních aditiv přidávaných do kostních cementů se zaměřením hlavně na polysacharidy.

V praktické části byly připravené cementy charakterizovány pomocí reologie, práškové rentgenové difrakce a statických zkoušek mechanických vlastností na samotném vytvrzeném cementu a slepených kostí. Reologie byla použita na měření rychlosti tvrdnutí cementu v závislosti na čase a teplotě. Dále byla taky reologie zamýšlena pro měření adhezivních vlastností roztoků kopolymeru, ale toto nebylo možné z důvodu nereprodukovatelných výsledků způsobené nehomogenitou roztoků kopolymeru s polysacharidem. Prášková rentgenová difrakce byla použita pro změření vlivu polysacharidu na konverzi fosforečnanu vápenatého na kalcium deficientní hydroxyapatit. Bylo zjištěno, že polysacharid významně neovlivňuje konverzi fosforečnanu vápenatého. Statické zkoušky mechanických vlastností byly použity pro změření maximální pevnosti v tlaku pro samotné vytvrzené cementové vzorky a také pro změření adheze slepených vzorků kostí. Vytvrzené vzorky s nízkou koncentrací polysacharidu vykazovaly vyšší pevnost v tlaku oproti kontrolním vzorkům. Při zkouškách kostí nebylo dosaženo průkazných výsledků z důvodu náročnosti měření. Jedná se zejména o přípravu vzorků kostí a jejich následné lepení kostním cementem.

KLÍČOVÁ SLOVA

Kostní cement, cement z fosforečnanu vápenatého, termosenzitivní kopolymer, polysacharid, reologie, adheze, prášková rentgenová difrakce, statické zkoušky mechanický vlastností.

SCHOLZ, David. *Vliv biopolymerů na adhezivní a reologické vlastnosti cementů z fosforečnanu vápenatého.* Brno, 2020. 59 s. Dostupné také z: https://www.vutbr.cz/studenti/zav-prace/detail/124850. Bakalářská práce. Vysoké učení technické v Brně, Fakulta chemická, Ústav fyzikální a spotřební chemie. Vedoucí práce Lucy Vojtová.

DECLARATION

I declare that the bachelor's thesis has been worked out by myself and that all the quotations from the used literary sources are accurate and complete. The content of the bachelor's thesis is the property of the Faculty of Chemistry of Brno University of Technology and all commercial uses are allowed only if approved by both the supervisor and the dean of the Faculty of Chemistry, BUT.

.....
student's signature

ACKNOWLEDGMENT

I would like to thank the head of my bachelor's thesis doc. Ing. Lucy Vojtová, Ph.D. for her professional guidance. Also, I would like to thank Ing. Matej Dzurov, Ing. Kristýna Valová and Ing. Jana Dorazilová for their valuable advice, consultations, willingness, and time. Furthermore, I would like to thank Ing. Petr Poláček, Ph.D. for his help with the mechanical tests, Ing. Klára Lysáková for synthesis of the copolymer and E. B. Montufar-Jimenéz, Ph.D. for preparation of TCP. Last but not least, I would like to thank MVDr. Edita Jeklová, Ph.D. from the VRI for her helpfulness by providing us with a dissecting room. And finally, I would like to thank my family for their support during my studies.

TABLE OF CONTENTS

1 INTRODUCTION

First calcium phosphate cements (CPCs) were developed in the 1980s and the first commercial CPC products were later introduced in the 1990s mainly for the treatment of maxillofacial defects and fractures. Since then, CPCs have gained increased attention and their formulations have been modified and improved in the past years and nowadays they can be used for applications such as bone augmentation, reinforcement of osteoporotic bones, fixation of metallic implants and vertebroplasty or kyphoplasty for spinal fractures [1]. The main component of CPC is calcium orthophosphate which forms a mouldable paste upon mixing with a liquid phase. When compared to acrylic bone cements, their main advantage is the ability to harden *in vivo* via a non-exothermic setting reaction under physiological conditions, whereas acrylic bone cement setting reaction is highly exothermic. Moreover, CPCs are suitable for bone repairing thanks to their excellent bioactivity, osteoconductivity, and also resorbability which depends on their composition. However, acrylic bone cements still have better mechanical properties and CPCs can be used only for moderate load-bearing applications and therefore, there is still plenty of room for improvement of CPCs formulations [2]. Current proven CPC formulation, composed of α-TCP as powder phase and thermosensitive copolymer solution as the liquid phase, lack sufficient adhesive properties. Chitosan is a biodegradable polysaccharide and has adhesive properties as a hydrogel, which could help to enhance the adhesiveness of CPC. This work aims to improve the adhesive behaviour by introducing chitosan into the original cement formulation.

2 THEORY

2.1 Bone

The human skeletal system consists of a total number of 213 bones and each of them undergoes modification during life to adapt to changing biomechanical forces and to remove old or damaged bone to replace it with a new and stronger one. Bones divide into four main categories which are long bones, short bones, flat bones, and irregular bones. The skeletal system fulfils a variety of functions. The most important function is the structural support for the whole body as well as facilitating movement and locomotion by serving as an anchor for the muscles. It also protects internal organs, serves as calcium and phosphate ions reservoir important for many metabolic functions, helps keep mineral homeostasis and acid-base balance. Bones are composite material formed by calcium phosphate and collagen [3], [4].

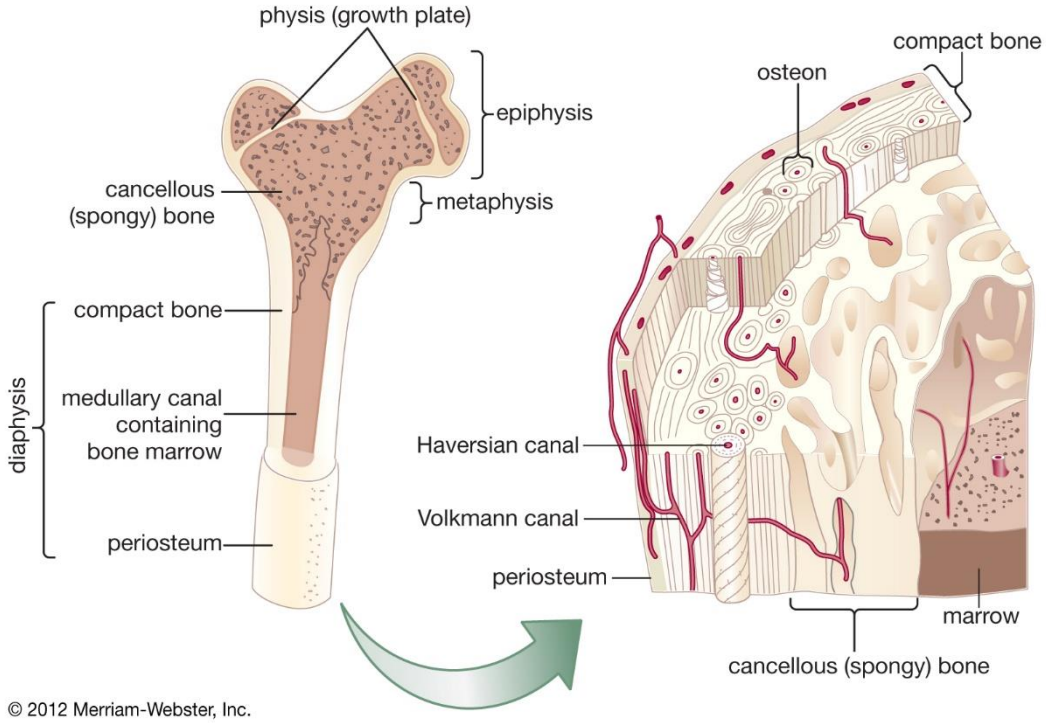

Figure 1: Internal structure of a human long bone [5]

As shown in Figure 1, long bones compose of three main parts: hollow shaft – diaphysis, cone-shaped metaphysis found below growth plates and above them are rounded epiphyses. The diaphysis consists mainly of compact cortical bone in contrast to metaphysis and epiphysis which is composed of spongy trabecular (cancellous) bone covered by a thin layer of cortical bone. Cortical bone forms 80 % of the adult human skeleton and the rest 20 % is trabecular bone. The ratio of these two types may differ with different sites within bones. For example, the vertebra has a ratio of cortical to a trabecular bone of 25:75, whereas the radial diaphysis has a ratio of 95:5. Cortical bone is compact and solid and surrounds the bone marrow compared to the trabecular bone which consists of honeycomb-like structure. Both bone types compose of osteons. Cortical osteons are called a Haversian system and trabecular osteons are called packets. Trabecular bone is usually more metabolically active than cortical bone [3].

Bones are renewed by remodelling process which main purpose is to retain bone strength and mineral homeostasis. The process is carried out by osteoclast and osteoblast cells. Hematopoetic osteoclast cells resorb old bone and stem cells-derived osteoblasts form a new bone. Essential bone building components are 80 to 100 nm thick mineralized collagen fibrils with a length to tens of microns. These fibrils compose of biological apatite and type I collagen. Whole bone consists of 50 to 70 % of mineral and 20 to 40 % of organic matrix. The rest is 5 to 10 % of water and less than 3 % of lipids. The mineral content is largely represented by hydroxyapatite $Ca_{10}(PO_4)_6(OH)_2$ with ionic substitutions and with a small addition of carbonate, magnesium and acid phosphate [3], [4].

2.1.1 Complications

The most common complication concerning bones is a fracture caused by trauma from direct forces in cases like falls or vehicle accidents but also from repetitive forces, for example in long-distance running, causing small cracks in bones which are called stress fractures. Other factors which can contribute to bone fractures are some disorders such as infections, bone tumours and most common osteoporosis [6].

2.1.2 Osteoporosis

Osteoporosis is a disease caused by loss of bone mass and structural degradation of bone tissue followed by the brittleness of bones with a higher risk of the hip, spine, and wrist fractures. Both men and women are affected by osteoporosis, but it can be prevented and treated. Women have less bone tissue, therefore, have a usually higher chance of developing osteoporosis than men. Greater risk also comes with age because bones become weaker. Other factors such as body size, ethnicity and family history can have an impact on developing this disease. Increased calcium and vitamin D intake, avoiding inactive lifestyle, cigarette smoking and excessive alcohol consumption can help as prevention [7].

2.2 Bone Repair

Worldwide, fractures connected with osteoporosis occur approximately to one in three women and one in five men with age older than 50 years. For example, approximately 2 million cases of bone fractures related to trauma or disease are yearly reported in the United States alone with an annual treatment cost of $10 billion. The repair rate of a fracture is affected by the wound size. The fibrous connective tissue becomes dominant in the site of fracture if the healing capacity of bone is not enough for the fracture size [2].

2.2.1 Bone Grafting

Bone grafting is used for traumatic bone defects and is considered to be adequate treatment. However, use of autologous bone grafts (iliac crest, rib, fibula) has a disadvantage in the form of morbidity, limited availability of material especially regarding older people and also possible post-operative complications [2], [8]. Many synthetic or biological materials have been studied in the search for an alternative to autologous bone grafts. With the increased interest in tissue engineering over the past years, approaches to bone grafting have improved significantly. The primary intention of tissue engineering based on scaffolds is to maintain normal function in the defected bone. Therefore, the main requirement for these types of bone grafts is the ability to

integrate with the host bone. Other obstacles are patients with age-related bone disintegration and already mentioned osteoporosis where bone repair using solid scaffolds may not be a viable approach. Thus, some orthopaedic and maxillofacial procedures prefer minimally invasive surgeries with the use of injectable bone cements (IBCs) [2]. For example, vertebroplasty and kyphoplasty where IBCs are injected directly to the vertebral body [9].

2.3 Injectable Bone Cements

Injectable bone cements can be classified as a group of materials consisting of powder and liquid phase. When these two phases are mixed, they create a plastic paste which is self-setting once implanted in the body. The paste consistency indicates that the material is mouldable and provide perfect fill in at the bone defect site and good contact between the material and bone even in complex defects. Ideal IBCs should fulfil a few important properties needed for its right function, which are listed below in Table 1. However, an ideal bone cement currently does not exist and all of them have certain limitations [9].

Table 1: Desired properties of IBCs [9]

- Ease of handling	- Low setting temperature	- No shrinkage during setting
- Injectability	- Near neutral pH during setting	- Appropriate mechanical strength
- *In vivo* setting with appropriate setting times	- No disintegration in early contact with body fluids	- No toxicity
- Biocompatibility	- Bioactivity	- Porosity
- High radiopacity		

IBCs can be divided into groups according to their chemical composition: Calcium phosphate cements (CPCs), acrylic bone cements (ABCs) and calcium sulfate cements (CSCs). Examples of setting reaction are shown in Figure 2. ABCs are mainly used for high and medium load-bearing applications, whereas CPCs and CSCs are usually used for medium and low load-bearing applications. CPCs are the main subject of this thesis and will be described in the following chapters [10].

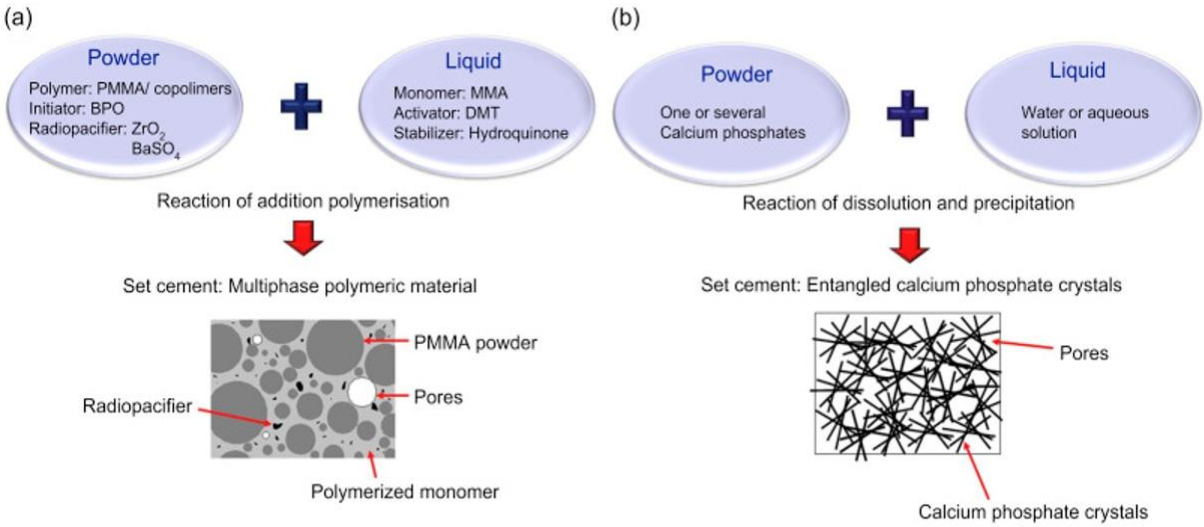

Figure 2: Difference between setting reactions of (a) ABC and (b) CPC [9]

2.3.1 Acrylic Bone Cements

ABCs main component is poly(methyl methacrylate) (PMMA) which has evolved from the use in ophthalmological and dental applications to orthopaedics as a material used for fixation of prosthetic implants for example in total hip, knee, ankle, elbow or shoulder joint replacements and also for remodelling osteoporotic, neoplastic, and vertebral defects [10], [11]. ABCs have proven valuable in implants fixation thanks to their good compression, shear, and tensile properties. Therefore, ABCs have better mechanical properties than ceramic CPCs. However, the disadvantage of PMMA is exothermicity during the polymerization reaction, which is shown in Figure 3. The polymerization reaction shown in Figure 2a generates heat and temperatures recorded by *in vivo* testing can reach a range between 40 and 56 °C which represent limit where values above could cause protein denaturation followed by related biological damage (osteonecrosis). Together with exothermicity, toxic monomers of PMMA are also a concern regarding ABCs biocompatibility. Also, PMMA is not bioresorbable [8], [11], but once it is cured, it shows non-toxic and biologically inert properties. Another drawback is prosthesis loosening which can come with time caused by the lack of secondary fixation or cement mechanical failure. Furthermore, particles and debris which could be released by the cement wear down may cause foreign body reaction inducing osteolysis [9].

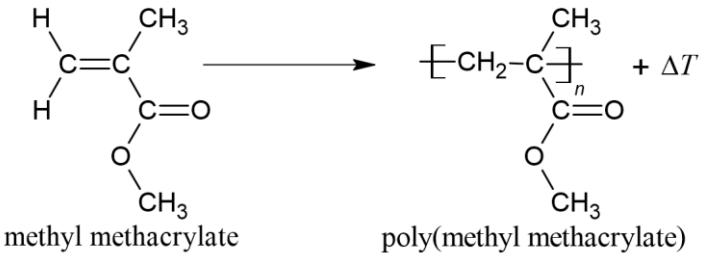

Figure 3: PMMA polymerization reaction

2.4 Calcium Phosphate Cements

First-generation biomaterials were mostly inert. In contrast, second-generation materials designed for orthopaedic applications are trying to aim to elicit a response from the body to

promote osseointegration, whether we are talking about mechanical fixation or replacement of diseased or injured bone. CPCs have been mainly used as second-generation biomaterials thanks to their chemical composition, which is similar to the natural bone indicating that the release of Ca^{2+} and PO_4^{-3} ions may have a positive effect on osteoconduction and osteogenesis. Moreover, degradation rates of calcium phosphates depend on their Ca/P ratio and the type of used filler [2].

2.4.1 Description

CPCs are hydraulic cements formed by mixing a powder phase, which consists of one or more calcium phosphates with liquid phase most commonly represented by water or aqueous solution. The formed paste is self-setting and hardening after being implanted in the body. In contrast to ABCs, which hardening is the result of the polymerization reaction, CPCs setting mechanism is based on dissolution and precipitation and entanglement of formed crystals as shown in Figure 2b [2], [9].

According to Figure 4, CPCs can be categorized either by the number of powder phase components to single or multiple or by the type of setting reaction to hydrolysis or acid-base reaction and finally by the type of end product to apatite or brushite cements [2]. The end product is usually characterized by the type of used calcium phosphate (CaP) solubility and reaction pH. When the pH value is greater than 4.2, hydroxyapatite (HA) or calcium deficient hydroxyapatite (CDHA) is formed with a poor crystalline structure. On the other hand, brushite also known as dicalcium phosphate dihydrate (DCPD) is formed within pH values lower than 4.2 [12].

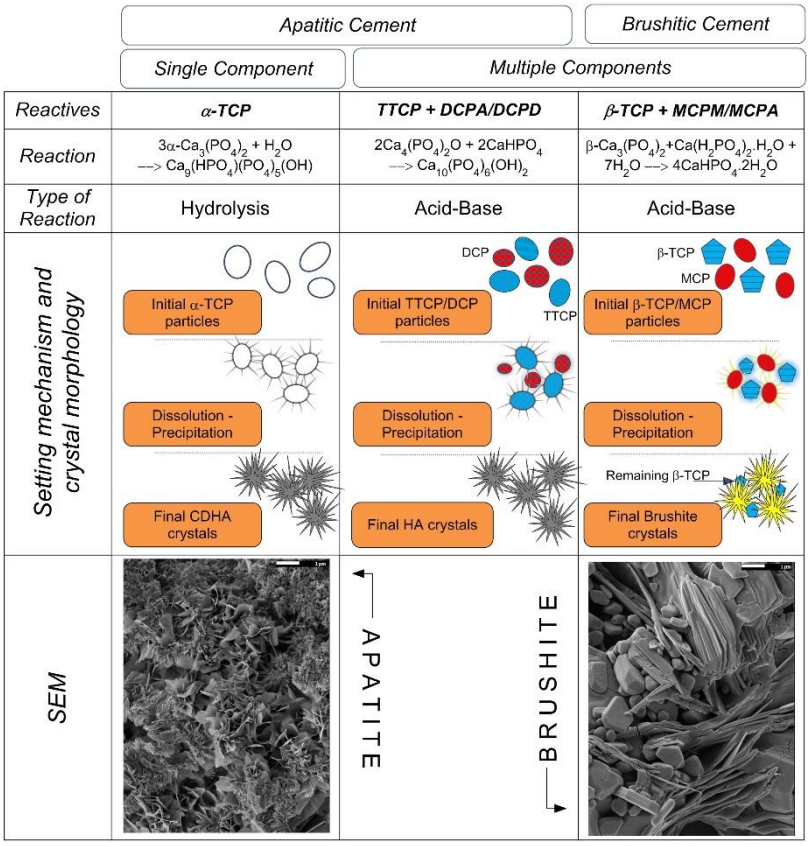

Figure 4: Setting mechanisms of different CPCs [1]

2.4.2 Apatite Cements

The product of apatite CPCs setting reaction and phase transformation is a poorly crystalline precipitated HA or also CDHA. The final composition of the product is a network of CaP crystals which is very similar to that of biological hydroxyapatite found in living bone and teeth. This is associated with the fact that apatite cements are formed in an aqueous environment, therefore, form a poorly crystalline structure [1], [12].

Tricalcium phosphate (TCP) and tetracalcium phosphate (TTCP) are among the most common precursors used for apatite cements [12]. As already mentioned, apatite cements can be categorized into two groups. Monocomponent CPCs use alpha tricalcium phosphate (α-TCP), which hydrolyses to CDHA according to equation 1 without the need to vary the Ca/P ratio [1].

$$3\ \alpha\text{-}Ca_3(PO_4)_2 + H_2O \rightarrow Ca_9(HPO_4)(PO_4)_5(OH) \quad (1)$$

In general, CPCs reactivity is affected by the particle size, degree of crystallinity and crystal phase. Smaller particle size provides a higher surface area which can react with the aqueous environment and increase the reactivity of the cement [12]. Higher reactivity can be observed with thermodynamically less stable CaPs. For example, amorphous calcium phosphate (ACP) is considered to be the least stable and therefore, the most reactive compared to α-TCP followed by β-TCP [1].

Multicomponent CPCs use two or more CaPs which some of them are more acidic and others more basic, this difference provides acid-base reaction as a setting mechanism as shown in equation 2.

$$2\ Ca_4(PO_4)_2O + 2\ CaHPO_4 \rightarrow Ca_{10}(PO_4)_6(OH)_2 \quad (2)$$

TTCP is usually the basic component and the second component is acidic CaP represented by dicalcium phosphate anhydrous (DCPA) or DCPD. The final Ca/P ratio of formed HA is given by the ratio of TTCP and the acidic component [1].

2.4.3 Brushite Cements

Brushite is metastable under physiological conditions compared to hydroxyapatite, therefore, brushite CPCs resorb much faster than apatite CPCs [1]. All brushite cements have DCPD as the final product of precipitation. In contrast to apatite cements, all brushite cements are formed by only the acid-base reaction. This is attributed to the fact that DCPD precipitates only in solutions with a pH less than 6. Most common formulation composes of β-TCP and monocalcium phosphate monohydrate (MCPM) which set according to the following equation 3 [12].

$$\beta\text{-}Ca_3(PO_4)_2 + Ca(H_2PO_4) \cdot H_2O + 7\ H_2O \rightarrow 4\ CaHPO_4 \cdot 2\ H_2O \quad (3)$$

Other formulations replace MCPM with phosphoric acid or use a combination of TTCP, MCPM and CaO. By replacing MCPM with phosphoric acid, several changes in cement properties occur: more control over the reaction and chemical composition; higher tensile strengths; prolonged setting time, which is welcomed change as brushite cements usually set

too fast from a liquid state. As already mentioned, they are highly bioresorbable and also biocompatible. Thus, brushite cements *in vivo* biodegradation is much faster than apatite cements. This is also connected with a rapid and significant decrease in mechanical strength after *in vivo* implantation. Furthermore, their setting reaction is more exothermic and due to the rapid setting times, a large volume of the liquid phase is needed to retain the injectability of the cement phase for a reasonable time. All of these disadvantages combined represent a limitation for the clinical applications specifically for load-bearing applications [9], [12].

2.4.4 Applications

Orthopaedic methods vertebroplasty and kyphoplasty have been developed to help treat vertebral compression fractures caused by osteoporosis. The goal of these procedures is to augment, stabilize and restore normal function and height to the defected vertebra. Both CPCs and PMMA cements can be used [12]. Using X-ray guidance, a thin needle cannula is inserted into the vertebral body and bone cement is injected under pressure through the cannula to the vertebra fracture site. Once the cement is injected, it hardens and provides stability for the fractured vertebra. The difference in vertebroplasty and kyphoplasty resides in that a balloon catheter is inserted into the vertebra using X-ray guidance again and it is inflated with a liquid under pressure. This helps to restore the vertebra fracture collapse and once the balloon is maximally inflated, it is deflated and removed leaving a cavity which is then filled with bone cement under lower pressure compared to vertebroplasty with the aim to maintain correction done by the balloon inflating [13].

Another application of CPCs is for maxillofacial and craniofacial procedures where the cement is stressed only moderately and therefore, CPCs are increasingly used in these types of applications. Moreover, good handling and ability to mould the material at the placement site is a great advantage from the surgical and cosmetic perspective. For example, CPCs have been used for the repair of neurosurgical burr holes, contiguous craniotomy cuts and cranial defects with a surface smaller than 25 cm^2. Friedman et al. reported repair of cranial defects for over 100 patients with approximately 97 % success rate after 6 years. Other applications involve hip fractures, fixation of bone screws and titanium implants, distal radius fractures and some dental applications [12], [14].

2.5 Calcium Phosphates

Calcium phosphates applications as bone repair materials have been studied for the last 80 years and their role in bone cements have been already described in the previous chapters. CaPs can be categorized in two types either as low-temperature CaPs which are obtained by precipitation from an aqueous solution at or around room temperature or as high-temperature CaPs which are obtained by a thermal reaction with the high temperature usually above 1000 °C [15]. The main parameters are the Ca/P molar ratio, basicity/acidity, and solubility. These parameters are associated with the solution pH. Lower Ca/P molar ratios mean that calcium phosphate is more acidic and water-soluble [16].

The most common CaPs are listed in Table 2, which shows the solubility range where high values are for acidic compounds such as MCPM and very low values are for basic compounds like apatites [16]. Hence low-temperature and high-temperature CaPs have different properties

and structure. The exception is stoichiometric hydroxyapatite (Ca/P 1.67) which can be precipitated at room temperature but is also stable to temperature up to 1300 °C. However, the distinction between this hydroxyapatite and the low-temperature form called CDHA, sometimes called precipitated HA abbreviated as PHA, must be made as their properties differ. CDHA is very similar to the mineral part of a bone, while HA is commonly applied in medicine. Another difference between CaPs types is their specific surface area. Low-temperature CaP such as CDHA can have a large specific surface area up to 100 m^2/g, whereas HA has a specific surface area of only around 1 m^2/g. This difference makes low-temperature CaPs much more reactive and biologically active compared to high-temperature CaPs [15].

Table 2: Most common calcium phosphates and their properties such as Ca/P ratio, solubility and pH range stability [16]

Name	Formula	Ca/P	Solubility[a]	pH[b]
(MCPM) Monocalcium phosphate monohydrate	$Ca(H_2PO_4)_2 \cdot H_2O$	0.5	~18	0.0–2.0
(MCPA) Monocalcium phosphate anhydrous	$Ca(H_2PO_4)_2$	0.5	~17	[c]
(DCPD) Dicalcium phosphate dihydrate	$CaHPO_4 \cdot 2H_2O$	1.0	~0.088	2.0–6.0
(DCPA) Dicalcium phosphate anhydrous	$CaHPO_4$	1.0	~0.048	[c]
(OCP) Octacalcium phosphate	$Ca_8(HPO_4)_2(PO_4)_4 \cdot 5H_2O$	1.33	~0.0081	5.5–7.0
(α-TCP) α-Tricalcium phosphate	$\alpha\text{-}Ca_3(PO_4)_2$	1.5	~0.0025	[d]
(β-TCP) β-Tricalcium phosphate	$\beta\text{-}Ca_3(PO_4)_2$	1.5	~0.0005	[d]
(ACP) Amorphous calcium phosphate	$Ca_xH_y(PO_4)_z \cdot nH_2O$	1.2–2.2	[e]	~5–12
(CDHA) Calcium-deficient hydroxyapatite	$Ca_{10-x}(HPO_4)_x(PO_4)_{6-x}(OH)_{2-x}$	1.5–1.67	~0.0094	6.5–9.5
(HA) Hydroxyapatite	$Ca_{10}(PO_4)_6(OH)_2$	1.67	~0.0003	9.5–12
(TTCP) Tetracalcium phosphate	$Ca_4(PO_4)_2O$	2.0	~0.0007	[d]

[a] Solubility at 25 °C, g/l.
[b] pH stability range in aqueous solutions at 25 °C.
[c] Stable at temperatures above 100 °C.
[d] Cannot be precipitated from aqueous solutions.
[e] Cannot be measured precisely.

2.6 Tricalcium Phosphate

Tricalcium phosphate $Ca_3(PO_4)_2$, also known under abbreviation TCP, is a white crystalline substance with three polymorphs. The first β-TCP is stable at low temperatures in contrast to the other two forms, α-TCP and α'-TCP, which are stable at high temperatures. Especially the α'-TCP exists only at temperatures higher than 1430 °C, therefore, this form does not have much utilization. α-TCP can be obtained by transformation of β-TCP by heating it to a temperature higher than 1125 °C and then the obtained α-TCP must be cooled down to room temperature. These two polymorphs are nowadays used in clinical applications in dentistry and orthopaedics. Although they have the same chemical composition, their properties like structure, density and solubility differ greatly. β-TCP is used for the preparation of biodegradable bioceramics, while α-TCP is the main component in calcium phosphate bone cements [17].

2.6.1 α-Tricalcium Phosphate

Differences between TCP polymorphs affect their chemical and biological properties, specifically solubility and biodegradability. α-TCP has a solubility of 0.24 mg/l at temperature 37 °C where on the other hand β-TCP has solubility only 0.15 mg/l at the same temperature. In general, concentration of Ca and P released from dissolution of calcium phosphates decreases in this order: TTCP > α-TCP > DCPD > DCPA > OCP > β-TCP > CDHA. Moreover, this order tells us that CDHA is the most stable of all listed calcium phosphates. Formation of CDHA is a result of dissolution and hydrolysis of α-TCP described by equation 1, which shows the fundamental principle of CPCs which set thanks to α-TCP conversion to CDHA in an aqueous environment [17].

2.7 Liquid Phase

The liquid phase usually consists of pure water, physiological saline solution or other aqueous saline solutions which mostly contain sodium phosphate salts [18]. Final properties of the cement paste-like viscosity, cohesion and washout resistance can be adjusted by modifying the liquid phase with the addition polymers, however, viscosities of most polymers decrease with increasing temperature but there are thermosensitive polymers which react the opposite way and undergo a sol-gel transition at a slightly increased temperature [19].

2.7.1 Thermosensitive Polymers

Thermosensitive polymers have gained increased attention and have been studied mainly for the use as drug delivery systems over the past years thanks to their sol-gel transition and formation of crosslinked hydrogels triggered by small temperature changes [20]. One of these polymers is poloxamer also referred to as pluronic which is amphiphilic triblock copolymer organized as ABA type composed of two polyoxoethylene (PEO) units and one central polyoxopropylene (PPO) unit. Sol-gel transition temperature can be modified by concentration and type of pluronic. The addition of pluronic improves injectability, cohesion and washout resistance of calcium phosphate cements [19]. However, pluronics are not biodegradable, and they are soluble only in physiological fluids with toxicity at higher concentrations [21].

Another thermosensitive polymer is also a triblock copolymer organized as ABA type where A block represents poly(lactic-co-glycolic acid) (PLGA) and B block represents polyethylene glycol (PEG). PLGA-PEG-PLGA copolymer commercially known as the ReGel® drug delivery system is soluble in water and thus, creates a free-flowing sol at or below room temperature but forms a hydrogel network at around body temperature depending on the copolymer solution concentration. These temperature transitions and thixotropic behaviour give the copolymer good injectability properties. Besides, the copolymer is approved by FDA, biodegradable and slowly degrades in the Krebs cycle to carbon dioxide and water. Compared to cement with water as the liquid phase, incorporating the copolymer into the cement formulation improves rheological aspects such as injectability depending on the concentration of the used copolymer solution. The copolymer acts as a surfactant and decreases the interparticle forces within the cement. In contrast, when water is used as the liquid phase, the α-TCP particles are subjected to attractive interaction forces which result in a stiffer material. The better injectability is also confirmed by lower yield stress which is required to start the injection. The yield stress of cement paste with water is three-time higher than that of the copolymer cement. Furthermore, the setting reaction is accelerated as the dissolution of the α-TCP is enhanced due to higher acidity of the copolymer solution (pH of 2.8) compared to pure water. When injected into water at 37 °C, cement mixed only with water disintegrates. In contrast, the copolymer cement exhibits better cohesion and washout resistance as it remains homogeneous. Good cohesion can be also observed by rheology measurements where the copolymer cement retains a high level of shear stress when shear strain is applied compared to cement with water which exhibits a significant decrease in shear stress once shear strain is applied. In addition, the copolymer cement does not show cytotoxicity in contact with human mesenchymal stem cells in a short-term period [20], [21].

2.8 Calcium Phosphate Cement Enhancing Additives

2.8.1 Gelatin

Gelatin is prepared either by thermal denaturation or physical and chemical degradation of collagen which is the main protein found in bone tissue. In medicine, it is widely used as hard and soft capsules, sealant, wound dressing, three-dimensional tissue regeneration, and surgical adsorbent. Gelatin aqueous solutions are in the sol state at temperature around 40 °C but once cooled down to room temperature they undergo gelification. Therefore, gelatin could improve mechanical properties and workability of the CPCs when added to the formula. Moreover, gelatin is fully biocompatible and completely resorbable *in vivo*. The organic gelatin and inorganic cement phase resemble composition similar to that of bone [22], [23].

Study of Bigi et al. showed that the presence of gelatin in the cement accelerates the setting reaction compared to the cements without gelatin. Furthermore, results showed that gelatin greatly improved mechanical properties with compressive strength values up to 14.0 and 10.7 MPa for the gelatin cements and 2.5-2.8 MPa for the pure cements. This is attributed to the fact that gelatin probably provides a better distribution of the mechanical load. Also, total porosity was reduced for the gelatin cement. However, this did not affect biological activity. On the contrary, the addition of gelatin positively affects osteoblasts viability and stimulated

collagen production [22], [23]. In their further research, they tried to incorporate small amounts of strontium which lead to better inhibition of bone resorption and osseointegration promotion without greatly changing the mechanical properties [24]. Unfortunately, no evaluation of adhesive properties was reported in these studies.

2.8.2 Fibrin

Fibrin plays an important role in blood coagulation where fibrin network is formed thanks to coagulation factors fibrinogen and prothrombin. This network structure prevents bleeding by the formation of a clot. The function of fibrin and the coagulation process can be mimicked by fibrin glue (FG) which is used to close wounds after surgeries and is commercially available. Hence, efforts have been made to combine the FG with CPC. The combination has proven in long-term clinical studies that FG positively improves early bone formation and angiogenesis. In the study of Lope-Heredia, long setting and fast setting FG powder components were combined with the CPC powder in a way so that a different volume of FG is formed in each sample and then mixed it with the liquid phase. The results showed that the FG network was well distributed, interconnected and had optimal porosity. Injectability and cohesion were also improved, however, with the increasing volume of formed FG in the samples, the mechanical properties decreased for both fast setting and long setting FG [25].

On the other hand, the study by Cui et al. also worked with FG but instead of mixing the FG with the cement powder, they prepared FG solution and then mixed it with the CPC powder in different powder to liquid ratios. The compressive strength declined with the decrease in the powder to liquid ratio for both FG and control specimens, but the compressive strength and elastic modulus were overall higher for CPCs with FG without significantly affecting setting time. Furthermore, good attachment and proliferation of bone marrow stromal cells were observed [26].

2.8.3 Alginate

Alginate is an anionic polysaccharide derived from brown algae cell walls. It is able to form hydrogels by absorbing water in up to 200 – 300 times its weight. It is biocompatible and forms gels through chelation mechanism with divalent cations. In most studies, the addition of sodium alginate increased setting times and also mechanical properties such as compressive strength and diametral tensile strength declined for various CPC formulations. Overall incorporation of sodium alginate did not improve the CPC properties [27]. However, the study by Lee et al. suggests otherwise. They used α-TCP as cement powder and 2% sodium alginate solution in 5% Na_2HPO_4 as the liquid phase. These two phases were mixed in different powder to liquid ratios. The results showed that sodium alginate decreased the setting time for all samples. The samples used for mechanical testing were soaked in a body simulating medium for 1, 3 and 7 days. Best results were observed for the powder to liquid ratio of 2.5:1 where both compressive strength and diametral tensile strength increased compared to the same sample but without sodium alginate [28].

In another study by Qi et al., soaking in PLGA polymer solution was used to enhance porous freeze casted sodium alginate CPC scaffolds. The incorporation of PLGA polymer into the scaffold macropores significantly improved mechanical properties. For 20% concentration of

the PLGA solution and CPC liquid to powder ratio of 3.25 ml/g, the compressive strength was 77 times higher than that of the alginate/CPC sample without PLGA [29].

2.8.4 Polydopamine

Marine mussels can attach on various solid surfaces in the sea thanks to their secreted proteins which contain 3,4-dihydroxy-L-phenylalanine (DOPA) and lysine. DOPA is a catechol containing compound and similarly, dopamine is a typical catecholamine which can form polydopamine (PDA) through self-polymerization in alkaline solution. PDA has great adhesive properties similar to that of DOPA due to high content of catechol groups which form covalent or strong noncovalent interactions with substrates. PDA is non-toxic, biocompatible and promotes adhesion and proliferation of osteoblasts. It has been used to modify biomaterials surface to improve hydrophilicity and biocompatibility and also to anchor nanoparticles, drugs, and proteins. Studies by Liu et al. showed that incorporation of PDA significantly enhanced compressive strength of CPC and promoted early HA conversion, but after 10 days of soaking, this conversion was inhibited compared to the control sample. PDA concentrated Ca^{2+} from the body simulating medium at the surface which mediated fast mineralization and formation of nanoscale HA layer. This layer had a high specific surface area which positively affected cells adhesion and proliferation. In their further research, they performed *in vivo* testing with rabbits where they implanted the PDA enhanced CPC to the femur, muscle and calvarial bone defects. Results showed improved bone repairing and biocompatibility and increased bone formation in PDA cements. Blood tests showed no significant increase in leukocytes and also no inflammation or necrosis was observed. Furthermore, push-out testing confirmed the early increase in bonding strength between implants and bone and XRD also confirmed that PDA inhibits the HA conversion. However, SEM images showed that lots of cells and tissue filled the interface between PDA cement and bone, whereas an obvious gap was observed for control cement [30], [31].

2.8.5 Sucrose Esters

Sucrose esters are prepared by trans-esterification of fatty acid esters with sucrose. The product of this reaction is a surfactant which splits in sugars and fatty acid upon hydrolysis. They are used as food additives (E 473) or in cosmetics. Surfactants have the ability to stabilize dispersions and since CPCs are concentrated dispersion of solid particles in aqueous solution, they could enhance the cement properties. Addition of sucrose esters to CPC formulation was done in the study by Bercier et al. which demonstrated improvement of adhesive properties and also injectability. Better adhesive properties were observed for hydrophilic sucrose esters. Addition of sucrose palmitate demonstrated the best adhesiveness depending on concentration and also showed good biocompatibility. Nevertheless, adhesive properties were measured for high concentrations up to 20 % and improvement in adhesion was not that significant for 1% concentration and moreover, their previous study showed that sucrose esters increase porosity of the cement and even 1% concentration of sucrose palmitate greatly decreased compressive strength from 12 to 4 MPa [32], [33].

2.8.6 Chitosan

Chitin poly(β-(1→4)-N-acetyl-d-glucosamine) (Figure 5) is after cellulose the second most abundant natural polysaccharide produced by a large number of living organisms and his solubility is very low in commonly used solvents. It can be found in the exoskeleton of arthropods or the fungi cell walls [34]. It was the first identified polysaccharide from mushrooms and was discovered 30 years earlier than cellulose. In 1859, C. Rouget performed first alkali treatment on chitin and created substance which could be dissolved in acids. Later in 1894, this deacylated chitin got name chitosan by Hoppe-Seiler [35].

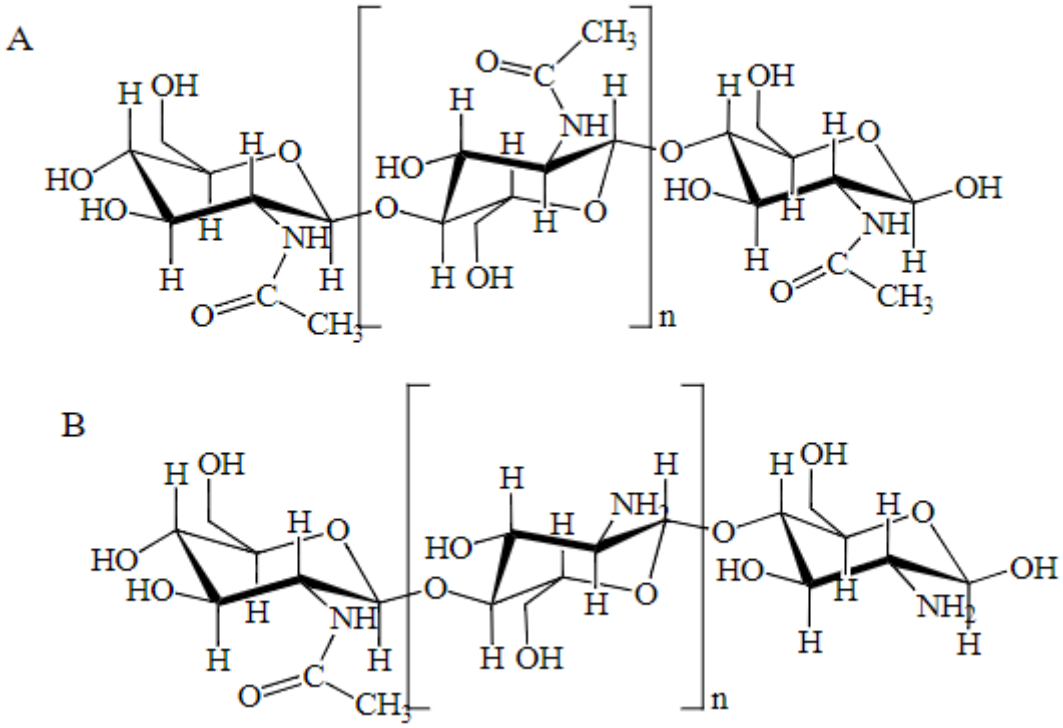

Figure 5: A chitin structure, B chitosan structure [36]

Chitosan (Figure 5) in solid form is a semi-crystalline copolymer [34]. It is a polysaccharide chain of N-acetyl-D-glucosamine and its deacetylated D-glucosamine units linked together by (1→4)-β-glycosidic bonds [37]. That indicates that chitosan is prepared by chitin deacetylation by alkaline hydrolysis of chitin acetamide groups. To obtain chitosan with a deacetylation degree (DD) higher than 70%, a strong alkali like sodium or potassium hydroxide and a high temperature of 100 °C are required [36]. Deacetylation degree and molecular weight (MW) of chitosan polymer have a big impact on its properties as shown in Table 3. Low molecular weight chitosan has usually molecular weight between 20 kDa and 190 kDa with DD lower than 75%, whereas chitosan with molecular weight ranges from 190 kDa to 375 kDa and has DD higher than 75% [37].

Table 3: Chitosan properties changes with deacetylation degree and molecular weight, ↑ means directly proportional and ↓ means inversely proportional [37].

Property	**Structural characteristics**		**Biological property**	**Structural characteristics**	
Solubility	↑DD		Mucoadhesion	↑DD	↑MW
Crystallinity	↓DD		Analgesic	↑DD	
Biodegradability	↓DD	↓MW	Antimicrobial	↑DD	↑MW
Viscosity	↑DD		Antioxidant	↑DD	↓MW
Biocompatibility	↑DD		Haemostatic	↑DD	

2.8.6.1 Properties

As already mentioned, chitin is mostly insoluble, but chitosan is soluble in diluted acidic solutions with pH lower than 6 thanks to amine groups with a pKa value of 6.3, which make chitosan soluble in water. Thus, chitosan solubility depends highly on pH which affects the charge of amino groups. At low pH, amino groups get protonated and gain a positive charge making chitosan cationic polyelectrolyte soluble in water. Contrarily, when pH is higher than 6, amines will deprotonate and loose charge making chitosan insoluble. This transition between solubility and insolubility takes place in a pH range between 6 to 6.5. As mentioned in Table 3, the deacetylation degree highly affects chitosan solubility. Also, molecular weight plays a significant role in solubility [37]. To achieve solubility in acidic solutions, chitosan with DD higher than 40% is required and solubility at neutral pH has also been reported with DD around 50%. Other factors that should be taken into account concerning solubility are ionic concentration and nature of protonation acid and distribution of acetyl groups in the polymer as well as intra-chain hydrogen bonds [34].

Chitosan aqueous solution with a neutral pH range from 6.8 to 7.2 has been obtained by adding glycerol-phosphate disodium salt to the solution which due to phosphate groups increases the pH of the solution. This results in liquid chitosan solution at neutral pH at room temperature but when the solution is heated to around 37 °C gel is formed with a significant rise of the elastic modulus (for pH 7.15). This sol-gel transition temperature is very dependent on pH and DD of chitosan [38].

Another important chitosan property is his biodegradability. Biodegradation of chitosan and polymers, in general, depends on their molecular weight. If the molecular weight is between 30 to 40 kDa, then it is suitable for renal clearance. Otherwise, the polymer will go through the degradation process. Chemical and enzymatic biodegradation should create fragments small enough, so they are suitable for renal clearance. In this case, chemical degradation means acid catalysed degradation as the one which takes place in the stomach. Enzymatically, chitosan is degraded by hydrolysis of glucosamine-glucosamine, glucosamine-N-acetyl-glucosamine, and N-acetyl-glucosamine-N-acetyl-glucosamine glycosidic bonds [39].

For example enzymes like lysozyme, papain and pepsin can degrade chitosan into non-toxic oligosaccharides with different chain length, which then can integrate into glycosaminoglycans and glycoproteins or to metabolic pathways or excretion [36]. It is easily hydrolysed by various chitosanases which are unfortunately completely absent in mammals [40]. In vertebrates, chitosan is primarily degraded by lysozyme and by certain bacterial enzymes in the colon [39].

Although humans do not synthesize or metabolize chitin or chitosan as a nutrient, our genome encodes 8 of 18 glycoside hydrolases family of chitinases (GH18) which hydrolyse the β-1,4-linkages in chitin, but only three of human chitinases have shown enzymatic activity [41]. However, not many information has been reported on the *in vivo* chitosan degradation, therefore, the degradation mechanism is currently not fully understood. Studies suggest that molecular weight plays an important role in distribution, degradation, and elimination process. The liver and kidney are considered as possible degradation sites based on localization of chitosan [37].

Chitosan is largely used in the development of delivery systems and has proved to be a safe excipient. It gained attention as a natural bioadhesive polymer with great mucoadhesive properties which can adhere to hard and soft tissues [37]. Clinical tests have shown no signs of any inflammatory or allergic reactions [40]. Also, more properties such as analgesic, antitumor, haemostatic, antimicrobial and antioxidant have been reported [36].

Chitosan analgesic effect has been studied by using an acetic-acid-induced writhing test in mice. Results showed that chitosan reduces inflammatory pain caused by intraperitoneal application of acetic acid. This effect is dose-dependent. Results indicate that the main analgesic effect is mediated by proton ions absorption released in the inflammatory site and also slightly by absorption of bradykinin which is a substance related to pain [42].

2.8.6.2 Hydrogel and Adhesive Properties

Adhesive behaviour in a liquid state is described by three main properties: the surface tension, the viscosity, and the ability of the adhesive to penetrate to the material. For a good molecular interaction, the adhesive surface tension must be lower or equal to the material surface energy. Low concentration chitosan solutions 0.5 % (w/v) have a surface tension of 64 mN/m which decreases over a long period to 41 mN/m. Solutions with higher chitosan concentration of 2 % (w/v) have an even lower surface tension of 37.4 mN/m. This low surface tension shows that it spreads well on most types of materials. Moreover, solutions with a concentration lower than 0.25 % (w/v) show Newtonian behaviour but above this concentration solutions have shear-thinning behaviour. Viscosity increases with concentration and decreases with temperature for example 4% (w/v) solution has a viscosity of 90.2 Pa·s in contrast to 9% (w/v) solution which has 7132 Pa·s at temperature 25 °C. Again, all properties depend on DD and molecular weight. 35 kDa and 350 kDa chitosan solutions viscosities were measured with the outcome of 3.2 Pa·s and 1085 Pa·s. Therefore, chitosan viscosity can be easily adjusted for its application which depends on the adhesive viscosity. Thus, this wide range of viscosities is an advantage when using chitosan as an adhesive [35].

Apart from use as a drug delivery system, another chitosan medical application is also as bioadhesive [35]. Bioadhesives are characterized as polymers with high molecular weight, biocompatibility, and biodegradability. They are used to join two material surfaces together where at least one of them is a living tissue to provide a substitute for surgical sutures [43]. One of the applications is related to its haemostatic properties. This allows materials based on chitosan to be used as emergency haemostasis and for skin wound closure. Wound closure is associated with chitosan great mucoadhesion in swollen state and its ability to adhere to hard and soft tissues. Chitosan films also support wound healing and tissue repair by adhering to fibroblasts and aiding the proliferation of keratinocytes resulting in better epidermal

regeneration [35]. Furthermore, anionic charges on erythrocytes in the blood react with chitosan polycationic charges and form a clot without the need of platelets or plasma clotting factor [44].

Hydrogels have several definitions, one of them defines them as macromolecular networks swollen in water or biological fluids. Based on the nature of this network, hydrogels are divided into three types, specifically entangled networks, covalently crosslinked networks and networks formed by secondary interactions [45].

However, when defining chitosan hydrogels, it is better to separate them as chemical and physical hydrogels. Chemical hydrogels same as covalently crosslinked hydrogels are formed by irreversible covalent links. On the other hand, physical hydrogels are similar to ionically crosslinked hydrogels and are formed by reversible links such as ionic interactions or secondary interactions. This type of hydrogel is easy to prepare by solubilisation of chitosan in an acidic aqueous medium. Entangled chitosan hydrogels lack mechanical strength and have a low tendency to dissolve therefore, their use is limited. Crosslinkers in hydrogels are molecules with MW much smaller than that of crosslinked chains. Formed hydrogels are highly dependent on properties like crosslinking density i.e. molar ratio of crosslinker to polymer repeating units. Furthermore, to form a hydrogel network, a critical number of crosslinks per chain is necessary [45].

Based on their structure, chemical covalently crosslinked hydrogels can be divided into three categories (Figure 6): chitosan crosslinked with itself, hybrid polymer networks (HPN) and semi/full-interpenetrating polymer networks (IPN). Chitosan crosslinked with itself have the simplest structure where two structural units are crosslinked with each other. When hydrogels are formed by HPN, the crosslink is between chitosan chain and a different polymeric chain. In case of semi/full-IPN hydrogels, a nonreactive polymer is added to chitosan solution before crosslinking. This results in entrapment of the nonreactive polymer into the chitosan crosslinked network and forms the semi-IPN gel. Besides, the nonreactive polymer can be further crosslinked to form two entangled crosslinked networks which are then considered as full-IPN gel whose properties can be different in contrast to semi-IPN gel. In all of these three cases, covalent bonds are the main type of bonds that form networks. Nevertheless, other interactions like hydrogen bonds and hydrophobic interactions cannot be excluded, but with increasing crosslinking density covalent become more predominant. Covalently crosslinked hydrogels can be used as drug delivery systems, implants, bandages, or scaffolds for cell culture growing [45].

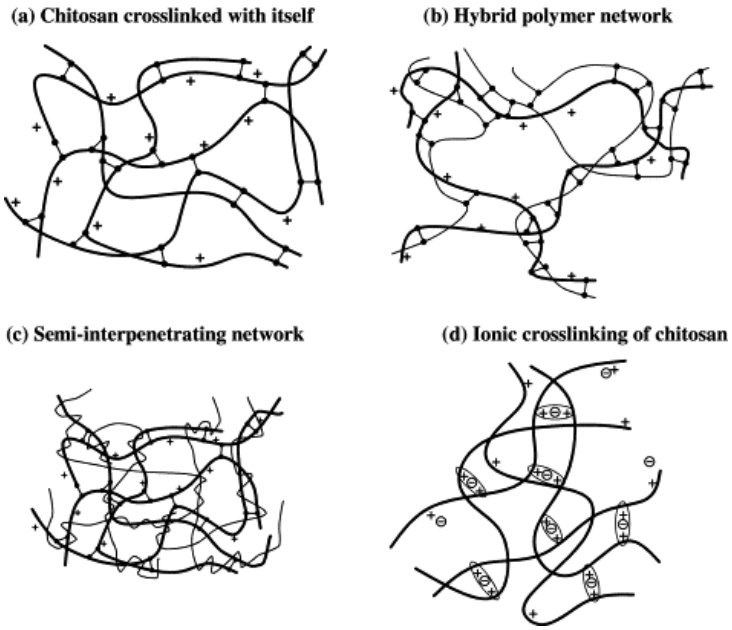

Figure 6: Various types of chitosan hydrogel networks [45]

The disadvantage of covalent crosslinking is the toxicity of most used crosslinkers. Hydrogels can be prepared by reversible ionic crosslinking to avoid a purification and verification process related to the use of a crosslinker. Chitosan is a polycationic polymer and thus, reaction with anions or anionic molecules provides a network of polymeric chains connected through ionic bridges (Figure 6d). In the case of chitosan crosslinking there is no need for polymers with a large MW distribution but only simple ions or ionic molecules with well-defined MW are used. Crosslinking density is again the main factor which determines properties such as mechanical strength and swelling. Hydrogels prepared by ionic crosslinking are mostly used as drug delivery systems as they lack the mechanical strength compared to covalently crosslinked hydrogels [45].

2.8.6.3 Applications in Calcium Phosphate Cements

Chitosan as the main subject of this work has been already described in the previous chapters and this chapter will deal with its application in bone cement. Researchers Yokoyama et al. developed CPC with incorporated chitosan and citric acid. The powder phase was composed of α-TCP and TTCP. The liquid phase composition was citric acid used in two different concentrations (20% and 45%), chitosan and glucose solution. The formed cement had good moldability and chewing-gum-like consistency. In general, cement with 45% citric acid concentration had higher compressive strength, but after 6 weeks the cement with 20% concentration had compressive strength 20.7 MPa in contrast to 15.6 MPa of that with 45% concentration. Furthermore, the inflammatory response was initially higher and longer for the cement with 45% concentration but disappeared over time for both concentrations. Thus, the concentration of citric acid has an impact on the mechanical properties and biocompatibility of the cement [46].

Another study from 1998 by Takechi et al. tested biocompatibility of anti-washout CPC with the addition of chitosan and conventional CPC mixed with citric acid or polyacrylic acid. Chitosan cement liquid phase had a concentration of chitosan 0.5 % and pH 7.4. Results showed

that chitosan cement had no inflammatory response compared to the conventional CPC and the one mixed with polyacrylic acid. XRD measurements showed that conversion to apatite occurred only for chitosan and conventional cement suggesting similar mechanical properties. In conclusion, this study demonstrated a good initial tissue response of chitosan cement, however, no evaluation of mechanical properties was reported [47].

In other studies, chitosan was substituted and added to CPC formulations. For example, Wang et al. used phosphorylated chitosan (P-chitosan) which is more water-soluble than unsubstituted chitosan in two different CPC formulations. The results showed an increase in compressive strength and Young's modulus for both formulations while setting time was slightly prolonged. This was dependent on deacetylation and substitution degree and MW of P-chitosan. The increase in mechanical properties was observed only to a certain limit of P-chitosan concentrations. Above this limit, the mechanical properties significantly declined and setting times increased. Further increase of P-chitosan concentration leads to no setting of the CPC at all [48].

Another substitute, chitosan malate was used by Sun et al. This substitute is again more water-soluble. The cement formulation was composed of TTCP and DCPA powder and liquid phase consisting of distilled water and chitosan malate added in mass fractions of 0, 10, 15, 20, 25 and 30 %. Best results were obtained with 20% mass fraction of chitosan malate compared to sample without chitosan. The cement setting time significantly reduced from 87 to 13 minutes. Furthermore, flexural strength increased from 4 to 14 MPa without greatly affecting resorbability, which was tested by *in vitro* dissolution experiment at various pH simulating *in vivo* environment [49].

Substitutes like chitosan acetate and chitosan lactate were also tested by Cherng et al. in CPC composed of TTCP and DCPA. However, the addition of these substitutes did not improve mechanical properties compared to the pure CPC [50]. This may be either attributed to the fact that these substitutes truly do not improve mechanical properties or that chitosan concentrations were too high as reported in the study with P-chitosan by Wang et al. Also, no information about deacetylation and substitution degree was listed in this study.

3 GOAL OF THE WORK

Current CPC formulation composed of α-TCP and PLGA-PEG-PLGA triblock copolymer does not present sufficient adhesive properties for the hardening cement. Chitosan as polysaccharide with good biodegradability and biocompatibility and also with slight adhesive properties which have been put to use for example in haemostatic bandages to cover wounds may provide these desired adhesive properties. Therefore, the goal of this work is to incorporate chitosan into the CPC formulation in different concentrations and evaluate its effect on the cement mechanical, rheological and adhesive properties.

The objectives of this work can be categorized in the following steps:

1. Rheological measurements to evaluate liquid phase properties and cement paste injectability and setting/curing behaviour viscosity and change of storage modulus in the cement paste over time at two different temperatures.
2. X-ray diffraction measurements to characterize phase composition and the cement setting kinetics.
3. Mechanical testing to evaluate the cured cement compressive strength and Young's modulus.
4. Mechanical testing of bone samples joined together by the cement to evaluate adhesive properties.

4 EXPERIMENTAL

4.1 Chemicals

- Poly(ethylene glycol) (PEG) (M_w = 1500 g·mol^{-1}) was purchased from Fluka (Switzerland)
- D,L-lactide (LA ≥ 99.9 %) was purchased from Polysciences (PA, USA)
- Glycolide (GA) (purity ≥ 99.9 %) was purchased from Polysciences (PA, USA)
- Tin octanoate (Sn(II) 2-ethylhexanoate 95 %) was purchased from Sigma-Aldrich (MO, USA)
- PLGA-PEG-PLGA copolymer (M_n = 5665 g·mol^{-1}, polydispersity index (PDI) = 1.090) was synthesised by Ing. Klára Lysáková (CEITEC – Advanced biomaterials)
- Calcium carbonate ($CaCO_3$ ≥ 99%) was purchased from Sigma-Aldrich (MO, USA)
- Calcium hydrogen phosphate ($CaHPO_4$ ≥ 98%) was purchased from Sigma-Aldrich (MO,USA)
- α-tricalcium phosphate (mean particle size 13.16 ± 3.78 μm) was synthesised by E. B. Montufar-Jimenéz, Ph.D. (CEITEC – Materials Characterization and Advanced Coatings)
- Liquid Nitrogen (LINDE company, Brno)
- Chitosan (medium M_w, degree of deacetylation (DD) 75-85 %) was purchased from Sigma-Aldrich (Germany) and used as received
- Gentamicin (concentration 1 mg·ml^{-1}) was purchased from B. Braun (Germany)
- Ultrapure water (ultrapure water of Type 1 according to ISO 3696)

4.2 Equipment

- Benchtop X-ray diffractometer (WAXS/WASD) (MiniFlex 600, Rigaku, Japan)
- Rotational Rheometer (AR-G2, TA Instruments, USA)
- Static materials testing machine (Z010 TE Allround-Line, Zwick/Roell)
- Incubator (CO2Cell 190 Standard, MMM-group, Germany)
- Cooled incubator (IL 68R, VWR® INCU-Line, Belgium)
- Digital microscope (Dino-lite AM7915MZT – Edge)
- Desiccator (SICCO, Germany)
- Millipore purification system (MilliQ Academic, Millipore, France)
- Analytical scale (AdventurerTM Pro, Ohaus, Switzerland)

4.3 Synthesis of the Thermosensitive Copolymer

The PLGA-PEG-PLGA triblock copolymer (ABA type) was prepared by Ing. Klára Lysáková using a conventional ring opening polymerization (ROP) method in a bulk nitrogen atmosphere. Briefly, poly(ethylene glycol), D,L-lactide and glycolide were homogenized at 130 °C and then injected with Sn(II)2-ethylhexanoate in PLGA/PEG weight ratio equal to 2.47 and PLA/PGA molar ratio equal to 2.96 as shown in Figure 7. The reaction proceeded for 3 hours. Then the product purification was performed by removing unreacted monomers by dissolution in cold

water and heating the solution up to 80 °C. The precipitated polymer was separated by decantation and dried in a vacuum oven at 30 °C to constant weight (for approx. 12 hours). The purification process was repeated three times [51].

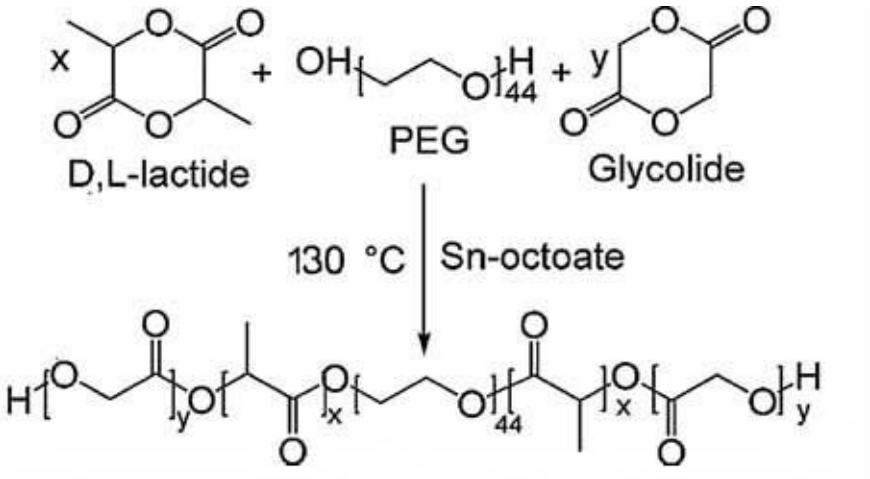

Figure 7: Synthesis of PLGA-PEG-PLGA triblock copolymer [51]

4.4 Synthesis of α-Tricalcium Phosphate

The α-TCP was prepared by E. B. Montufar-Jimenéz, Ph.D. as follows. A stoichiometric mixture of calcium carbonate and calcium hydrogen phosphate was used to synthesize α-TCP in a furnace at 1400 °C. Then quenching was performed to stabilize the alpha phase. Obtained α-TCP was dry milled in a planetary mill using an agate jar and balls. First milling was performed using 10 balls (d = 30 mm) for 60 minutes at 450 rpm and the second milling using 100 balls (d = 10 mm) for 60 minutes at 500 rpm to obtain a fine powder [52].

4.5 Samples Preparation

PLGA-PEG-PLGA triblock copolymer solution was prepared by weighing the copolymer to a glass vial and adding ultrapure water to obtain 15% w/v solution. Dissolution was performed at low temperature using a cooled incubator with a magnetic stirrer for 3-5 days.

After sufficient dissolution of the copolymer, the α-TCP powder was weighed according to liquid to powder ratio of 0.5, where the liquid is represented by the ABA triblock copolymer solution. Before mixing the two phases, tube forms around 6 mm in diameter and 12 mm long were cut from a PVC tube. These forms were then placed to a rubber plate with holes of the same diameter in a petri dish. This whole form assembly was sanitized with ethanol before using it. Then the powder phase was added to the liquid phase and the mixture was stirred. The resulting cement paste was loaded into a syringe and injected into the prepared forms carefully to prevent uneven distribution of the cement. The filled forms were consecutively placed into the incubator environment with 100% humidity and temperature 37 °C and were left to set for a certain time according to need of individual measurement.

After sufficient dissolution of the ABA triblock copolymer, solid chitosan was weighed and added to the solution to obtain 0.5%, 1% and 2% w/w concentrations of chitosan. Then the chitosan was left to properly dissolve and the solution was used as a liquid phase and the following process was the same as mentioned above. To make it simpler CPC samples will be

further referred to as CS0, CS0.5, CS1 and CS2 for each chitosan concentration, respectively, where CS0 are control samples without addition of chitosan.

4.6 Bone Samples Preparation

This part of the work was performed in cooperation with VRI (MVDr. Edita Jeklová, Ph.D.) in Brno which provided us with a dissecting room. Three porcine femur bones were used to prepare samples. Using a hand bone saw, both femoral epiphysal condyles were sawn off to obtain a 10 cm long diaphysis. Both bases of the bones were ground using sandpaper to make them as parallel as possible and then the bones were sawn in the middle under 45° angle as shown in Figure 8,A. The cross-sections sawn under angle were scanned using a digital microscope to calculate the surface area of cortical bone using ImageJ software. Afterwards, a cement paste was prepared according to the previous chapter in concentrations CS0, CS0.5 and CS1 and approximately 1 ml of the cement paste was applied only to the cortical bone surface of a one half of the bone and the second half was attached to it (Figure 8,B) and wrapped with gauze to prevent it from sliding. The glued bones were then submerged in a PET bottle with approximately 600 ml of physiological solution and 2 ml of antibiotic Gentamicin to prevent rotting. All PET bottles were submerged in already tempered 37 °C water bath. Samples were left to set for one day and consecutively used for the adhesion measurement.

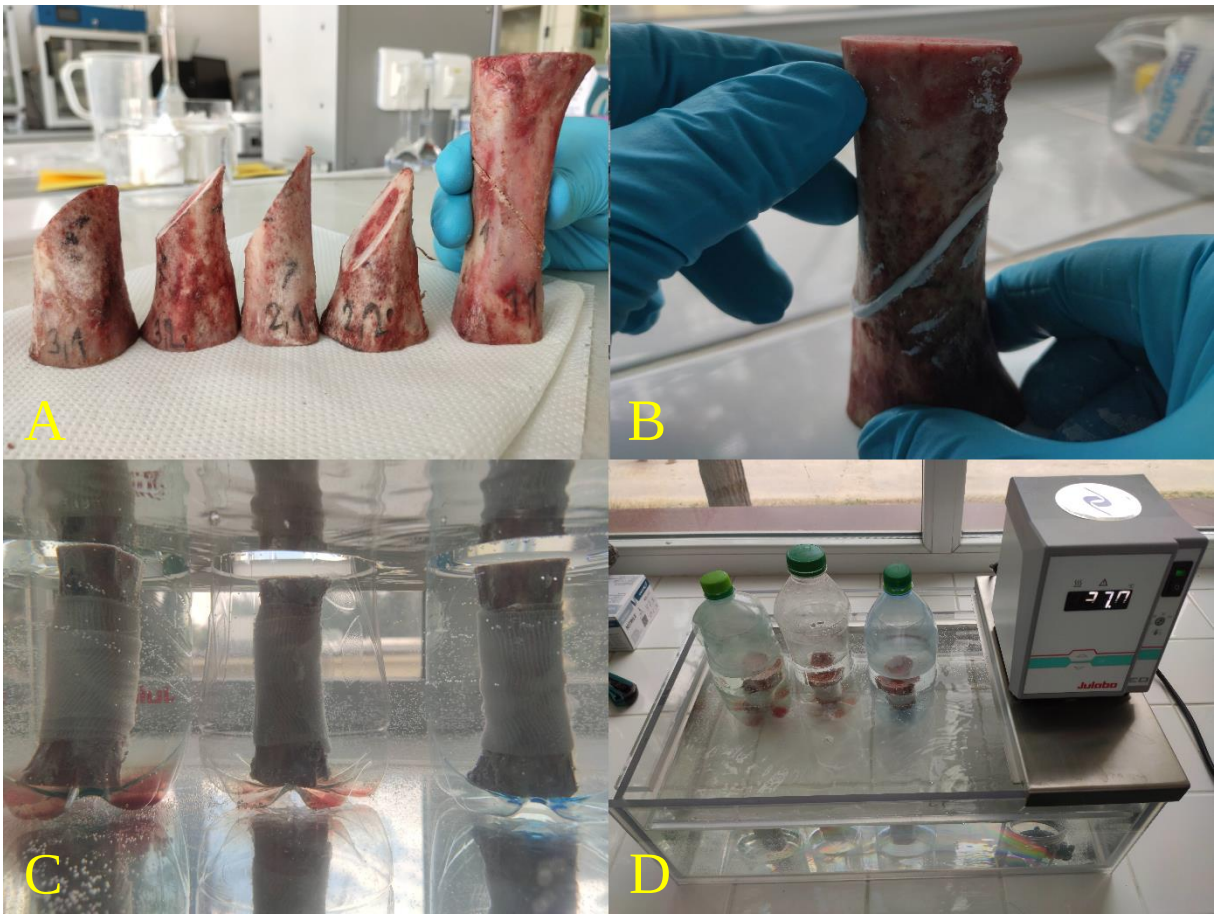

Figure 8: A: porcine femoral bones cut under 45° angle, B: two cut bones joined together by cement paste, C,D: water bath setup with the glued bones placed in PET bottles

4.7 Powder X-ray Diffraction Measurement

X-ray diffraction is described as the elastic scattering of X-ray photons by atoms which form a periodic lattice. When the scattered monochromatic X-rays are in phase, they give constructive interference. Conversely, if they are not in phase, they give destructive interference. Thanks to this diffraction by crystal planes we are able to derive lattice spacing using the Bragg's law defined by equation 4 [53].

$$n\lambda = 2d \sin \theta \tag{4}$$

Where n represents the order of reflection, λ is the wavelength of X-rays, d is the specific spacing between each crystal plane and θ is the angle between the incident or reflecting X-ray beam and the crystal lattice plane. Therefore, by measuring the reflected X-rays beams which interfere constructively, it is possible to measure lattice spacings of every single crystallographic phase. To identify an unknown sample, the recorded diffraction patterns are compared with the standard patterns in the database [53]. However, in this work, external standard method was used for measuring the kinetics of the setting reaction to monitor the conversion of α-TCP to CDHA where pure α-TCP was used as standard thus a simple comparison of peaks patterns was sufficient. Specifically, conversion can be observed from the decrease in intensity of 2θ angle peak of 30.74°.

In general, samples were prepared according to chap. 4.5 and were left to set for a different amount of time. The samples were then ground to obtain the finest powder possible using mortar and pestle. Powdered samples were then loaded onto a glass holder and inserted into the benchtop X-ray diffractometer (WAXS/WASD) (Rigaku, MiniFlex 600) and measured. Samples were measured in continuous mode in 2θ angle range from 5 to 50 degrees with step 0.02 degree and speed 20 degrees/min. X-ray generator output was 600 W (40 kV, 15 mA) with Cu target.

First set of control CS0 CPC samples were left to set for 1, 3, 5, 7, 10 and 12 days. These samples were used to measure the kinetics of the setting reaction to evaluate conversion of α-TCP to CDHA and establish a suitable setting time for mechanical testing. The second set of CS0, CS0.5, CS1 and CS2 samples were left to set for 0.5, 1, 1.5, 2, 3, 4 and 5 days and were used to determine the early conversion of α-TCP to CDHA with the addition of chitosan.

4.8 Measurements under Compression

Tests under compression were used to determine material behaviour under applied crushing loads. They are usually performed by applying compressive pressure to cylindrical test specimens using special geometry such as plates or other accessories on a universal testing machine. The outcome of these tests is a stress-strain diagram from which properties such as compressive strength or Young's modulus are determined. Compressive strength is the maximum stress that a material can sustain under crush loading before shattering [54]. Young's modulus is a specific form of Hooke's law which tells us that small deformations of an object are directly proportional to the applied force. Therefore, Young's modulus is only appliable when stress is proportional to strain, the course of the stress-strain diagram is linear, and the

deformation of a material is not permanent. It is used to describe the elastic properties of a material under tension or compression in only one direction [55].

CPC samples were prepared according to chap. 4.5 and were left to set for 10 days. Then they were cut out from the PVC forms using a scalpel and their cylindrical bases were adjusted to be as much parallel as possible using sandpaper. Afterwards, their dimensions were measured using digital calliper ruler and samples were ready to use for compressive strength measurement. Measurement was performed using static materials testing machine (Z010 TE Allround-Line, Zwick/Roell) with 1 kN load cell. 10 g pre-load was applied and strain controlled deformation speed of 1 %·min^{-1}. This method was also used to evaluate adhesion strength by measuring the compressive strength of glued bones with 100 kN load cell and the same conditions as mentioned above.

4.9 Rheology Measurement

Rheology is a method used to describe the deformations and flow behaviour of materials with a wide range of viscous or viscoelastic properties from liquids like water to gels and solid materials like metals. The basic principle of rotational rheology measurement is that the lower geometry is stationary, and the upper geometry rotates and applies a shear force upon the sample between these two geometries. The most common geometries for rotational rheometers are plate-plate and cone-plate. Continuous rotational tests are used to measure viscosity and to determine if the liquid has Newtonian or non-Newtonian character. The measurement is usually performed in ramp modes where either shear rate or shear stress is gradually increasing or decreasing. Oscillation tests are used to measure viscoelastic properties of more solid-like materials where the upper plate is not continually rotating but oscillating by moving back and forth. Shear stress is applied to the material which results in shear deformation. These two values are important to evaluate storage modulus G' and loss modulus G''. Storage modulus provides information about the elastic part of the viscoelastic behaviour which describes the solid-state behaviour of the sample, whereas loss modulus represents the viscous part of the viscoelastic behaviour which describes the liquid-state behaviour of the sample. This method was used to determine the viscosity of liquid phases used for the preparation of CPC samples and then to evaluate the change of viscoelastic behaviour during setting of the CPC samples in time at different temperatures [56]. Furthermore, rheology parameters correlate with adhesive properties to some degree. This method cannot be used to measure the adhesion directly but only to compare it between samples from differences in moduli. Storage modulus correlates to cohesive strength, whereas loss modulus correlates to adhesive strength. If loss modulus value is high at high oscillation frequency, then it indicates high peel strength at the interface and on the other hand, if the value is low at low oscillation frequency, then it indicates high adhesion shear resistance at the interface. Therefore, the method was used to compare the adhesive properties of chitosan samples to the control sample [57].

Samples were measured using a rotational rheometer (AR-G2, TA Instruments, USA) with a plate to plate geometry with 20mm plate and Peltier unit to maintain a constant temperature during the measurement. The liquid phases CS0, CS0.5, CS1 and CS2 were prepared according to chapter 4.5 and measured in a liquid state by steady-state flow method with shear rate a range from 0.1 to 100 s^{-1} and 1000 μm gap for the viscosity measurement and then by frequency

sweep method at temperature 37 °C in frequency range from 0.01 to 90 Hz with strain 1 % and 500 μm gap to measure adhesive properties.

The CPC samples were prepared according to chap. 4.5 but were used for measurement as a paste directly after mixing the liquid and powder phases by a time sweep method for one hour at temperature 23 °C and then for four hours at temperature 37 °C, both under constant parameters with 0.01 % strain and frequency 1 Hz and 1000 μm gap.

5 RESULTS AND DISCUSSION

5.1 Preparation of Liquid Phase

Liquid phase containing only ABA copolymer was free-flowing and thus easy to manipulate with. Addition of chitosan in different concentrations to the copolymer solution resulted in an increase of viscosity to almost gel-like consistency and the solution was not as free-flowing as pure copolymer solution which sometimes made the solution non-stirrable using a magnetic stirrer. This change was observed most intensively for liquid phases of CS0.5 and CS1 samples where the solution was not free-flowing at all and more viscous. Liquid phase of CS2 sample was less viscous and more free-flowing than CS0.5 and CS1 samples but still not as much as pure copolymer solution. However, the higher the concentration of chitosan was, the more difficult it was to dissolve the whole amount of chitosan and for CS2 sample, small pieces of undissolved chitosan could be sometimes observed. These observations correlate with rheology results where the viscosity of the copolymer with chitosan was measured by steady-state flow method. Figure 9 shows that the highest viscosity was measured for CS0.5 and CS1 samples with almost the same values and then a decrease can be seen for CS2 sample. As expected, the lowest viscosity was measured for control CS0 sample.

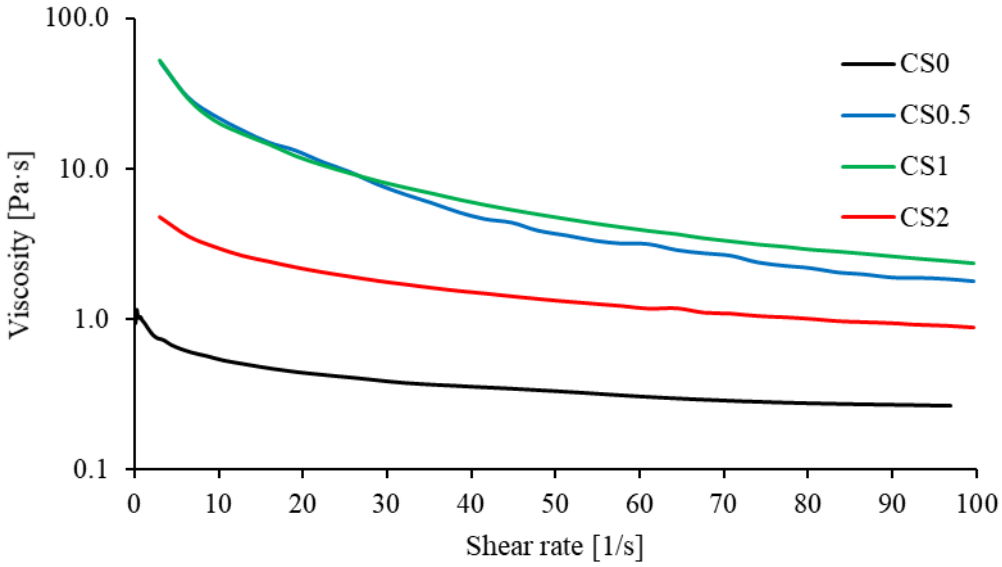

Figure 9: Viscosity measurement of the copolymer with chitosan by steady-state flow method

5.2 Evaluation of Rheological Aspects

5.2.1 Liquid Phase

Firstly, a strain sweep of CS0 and CS1 sample was performed to evaluate strain value for frequency sweep which would correspond to the linear viscoelastic region. The LVE region indicates the range in which the test can be carried out without destroying the structure of the sample. The results are shown in Figure 10 from which a strain 1 % was chosen for further frequency sweeps as it corresponds to the linear viscoelastic region.

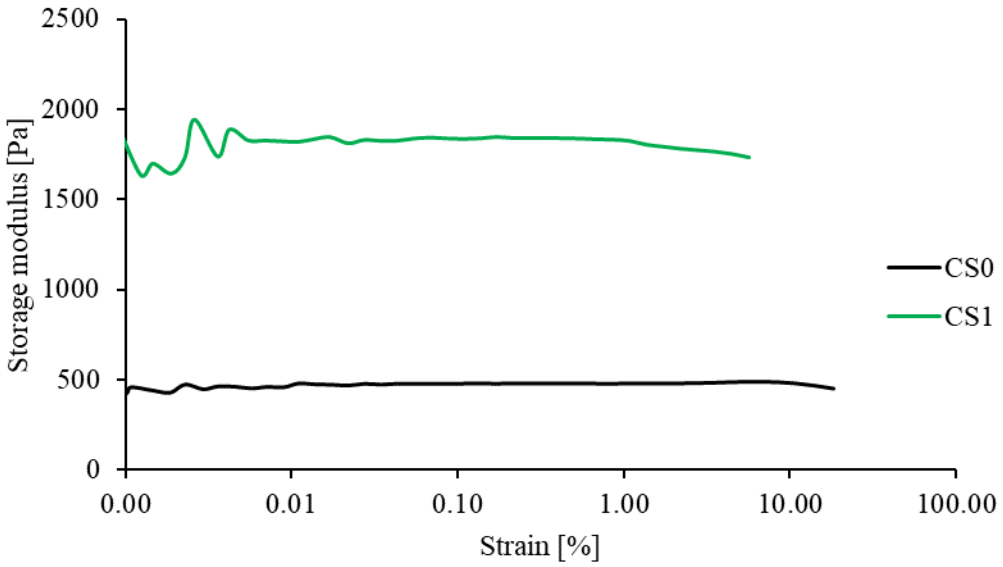

Figure 10: Stress-sweep measurement of CS0 and CS1 copolymer solutions

Figure 11 shows results from measuring the CS0 sample in frequency sweep mode. The measurements had a similar course and showed that the sample can be measured reproducibly which proved the correct setting of the measurement. However, when compared to results from measuring the CS1 and CS2 samples in frequency sweep mode under the same conditions, which are shown in Figure 12 and Figure 13, respectively, it is evident that samples cannot be measured reproducibly as each measurement had a different course.

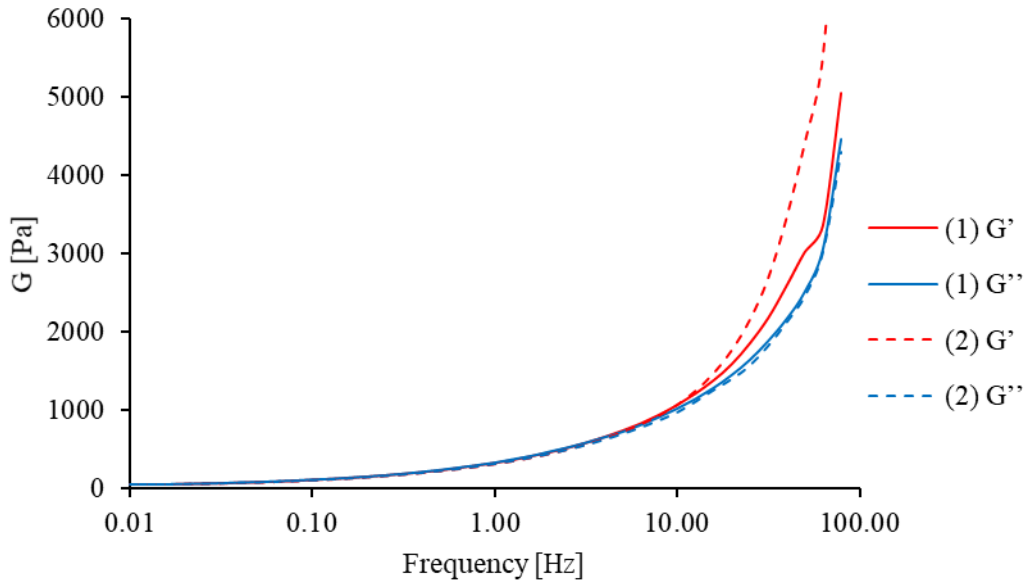

Figure 11: Frequency sweep of CS0 sample (magnetic stirrer)

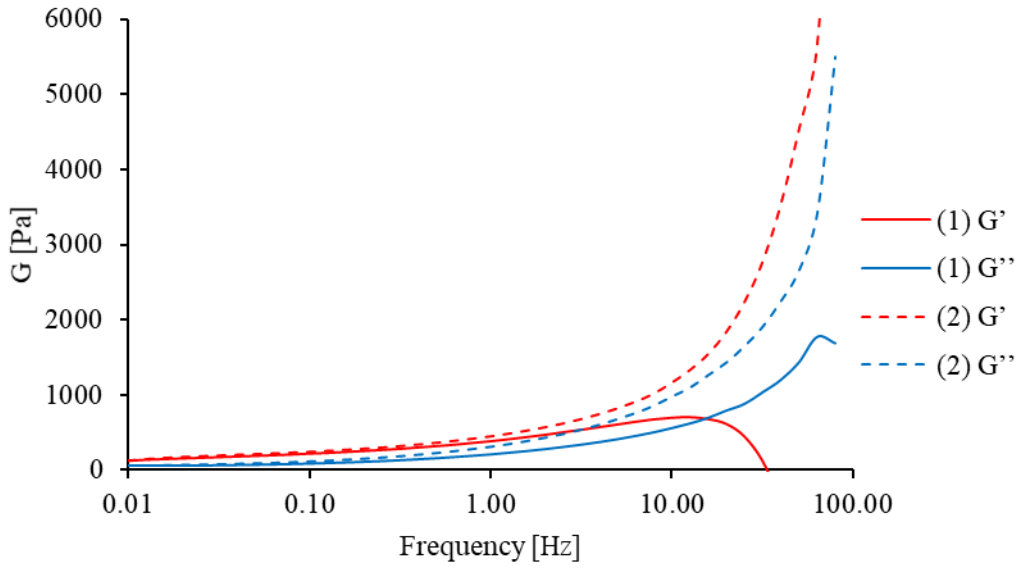

Figure 12: Frequency sweep of CS1 sample (magnetic stirrer)

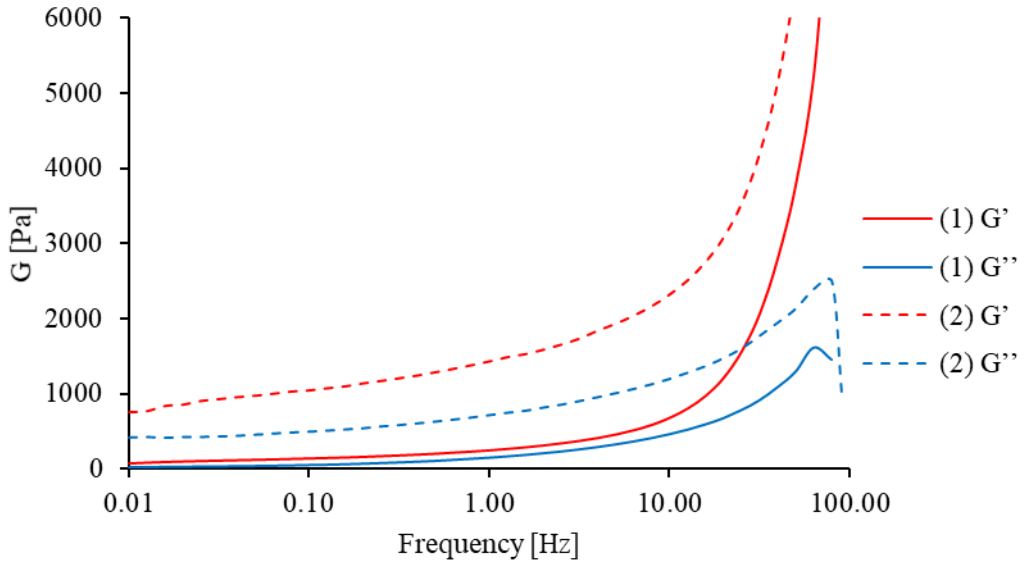

Figure 13: Frequency sweep of CS2 sample (magnetic stirrer)

It was found out that the non-reproducibility was caused by inhomogeneity of the chitosan copolymer solutions due to foaming and bubbles which formed during the preparation of the solutions. These samples were prepared using a magnetic stirrer and therefore a different method of preparation was tested to see if we could get rid of the bubbles. Next set of samples were prepared by dissolving chitosan in the copolymer solution by centrifugation which removed the bubbles and samples were measured under the same conditions again. Figure 14 shows that the measurement was also non-reproducible and therefore other samples were not even measured. The samples were then put under a digital microscope which revealed the core of the problem. Figure 15 shows that the CS0 sample was homogeneous and thus the measurement was well reproducible. Centrifugation removed the bubbles, however, another problem remained in the form of insufficient dissolution of chitosan particles. Preparation using

magnetic stirrer seemed to have better chitosan dissolution, but the bubbles represented a major complication. Due to these complications, the mentioned method to evaluate adhesion properties could not be applied. Moreover, It was also found out that the behaviour of the copolymer solution with chitosan is highly dependent on the method of preparation and hence a greater effort must be put to find and optimize the right preparation method with ideal conditions. Some recommendations are presented in chapter 6.

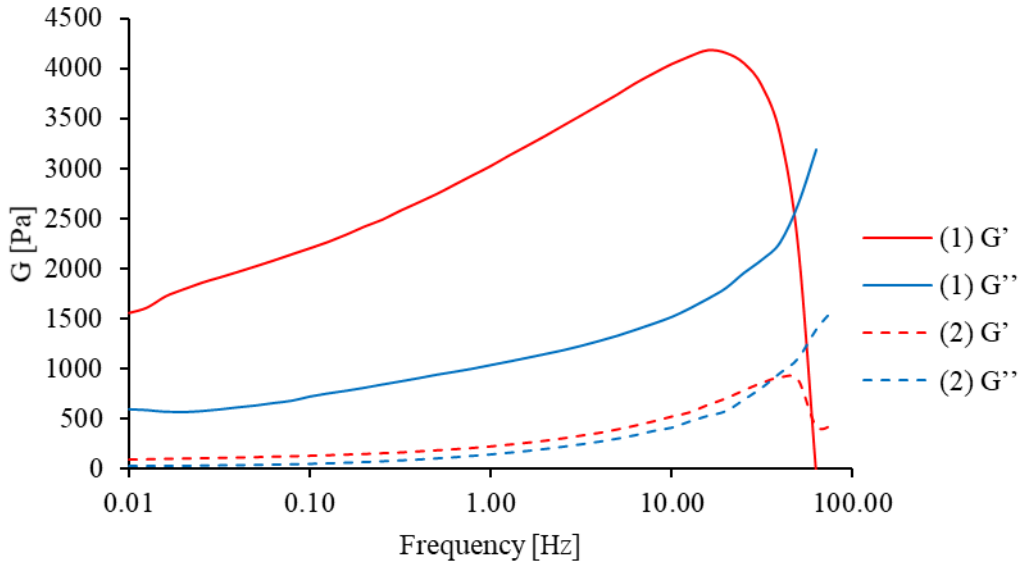

Figure 14: Frequency sweep of CS2 sample (centrifugation)

Figure 15: Copolymer solutions prepared in different ways, from left to right: pure CS0 solution (magnetic stirrer), CS2 solution (magnetic stirrer), CS2 solution (centrifugation)

Although the measurements could not be reproduced and the adhesive properties could not be evaluated as originally intended, some adhesive behaviour was observed for the chitosan samples after the measurements as shown in Figure 16. When the geometry was lifted, the samples adhered to the upper geometry. This was observed only slightly for CS0.5 and CS1 samples but the CS2 sample coated the upper geometry whole surface indicating a cohesive failure instead of adhesive failure and therefore, CS2 sample may possibly have better adhesive properties. Nevertheless, this is only an assumption and further research is needed.

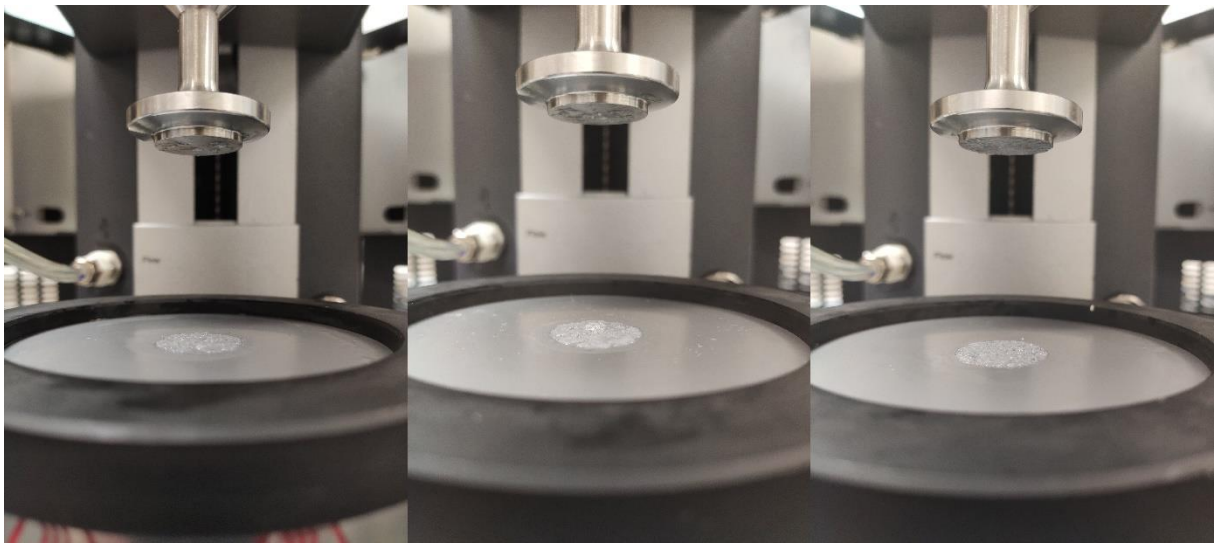

Figure 16: Samples after the frequency sweep measurement, from left to right: CS0.5, CS1, CS2

5.2.2 Calcium Phosphate Cement Paste

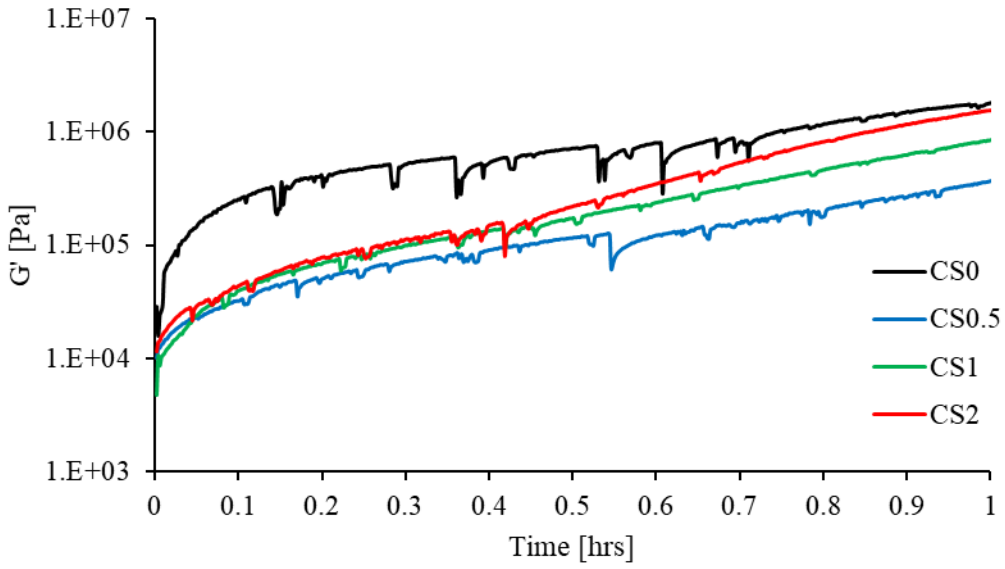

Figure 17: Time sweep measurement at temperature 23 °C for one hour

Results from the measurement at temperature 23 °C for one hour are shown in Figure 17. The gradual increase in storage modulus is caused by the conversion of α-TCP to CDHA. Compared to CS0 sample, the highest decrease in storage modulus was observed for CS0.5 sample and then the decrease was gradually smaller with higher chitosan concentration. The smallest decrease was thus observed for CS2 sample. This indicates that small addition of chitosan improves flow and viscous properties of the cement paste, however, with increasing chitosan concentration, this trend is declining same as compressive strength. Although all samples were easily injectable through a syringe, this shows that chitosan could slightly improve the injectability. A similar trend was also observed for the measurement at temperature 37 °C for four hours and samples with higher chitosan concentration hardened faster. Figure 18 shows that CS0.5 sample had the lowest increase and overall storage modulus compared to other samples. CS2 sample had almost the same setting course and storage modulus as control CS0

sample and surprisingly CS1 sample had a slightly different course than other samples. Storage modulus was constantly increasing until the sample was completely hardened and geometry lost contact with the sample. This deviation from other samples was initially considered as measurement error, however, the second measurement truly confirmed the constant storage modulus increase. Similarly, the same happened for CS2 sample and after approximately three hours, the sample was also hardened as shown in Figure 19 and could not be further measured. This indicates that CS1 concentration is more suitable for bone glue application than the others as it sets faster which is welcomed attribute.

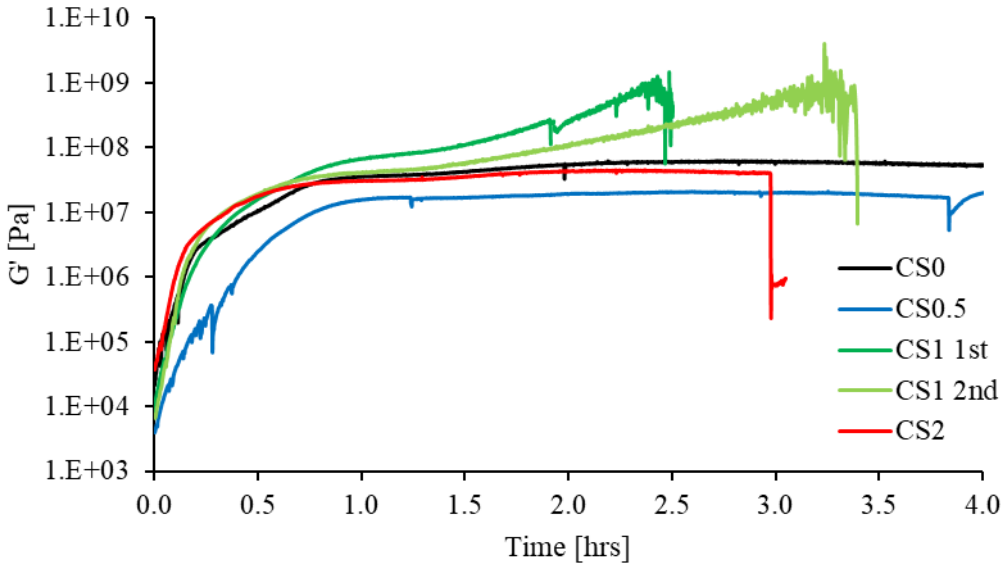

Figure 18: Time sweep measurement at temperature 37 °C for four hours

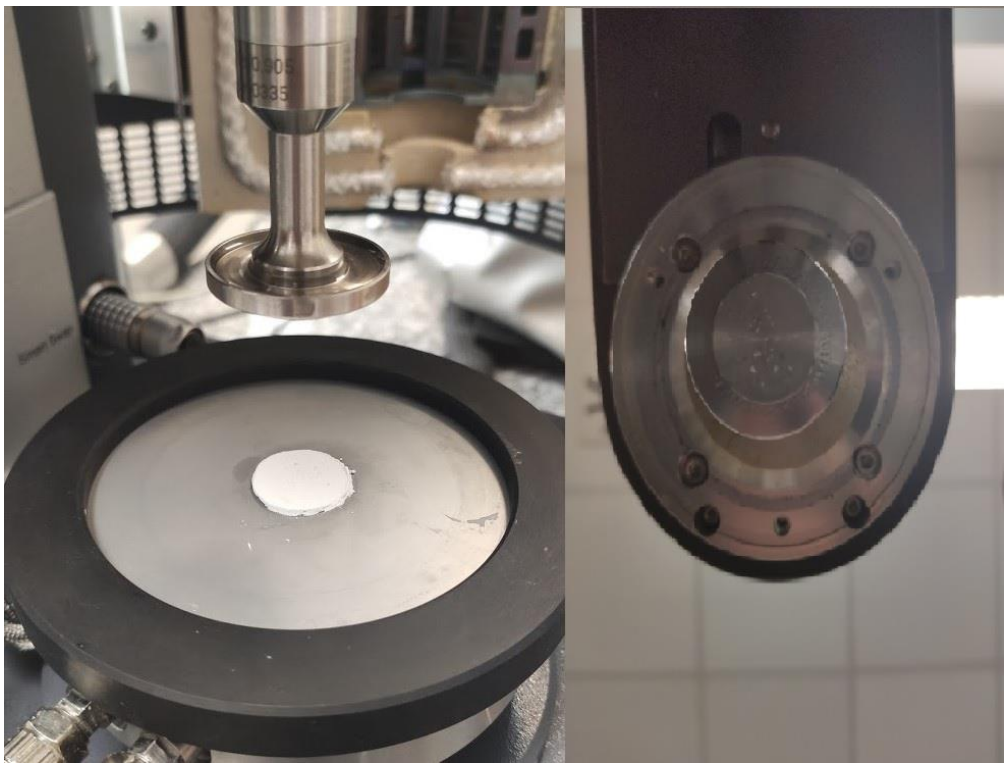

Figure 19: Left: hardened CS2 during measurement at 37 °C, right: the geometry bottom view

5.3 Powder X-ray Diffraction Results

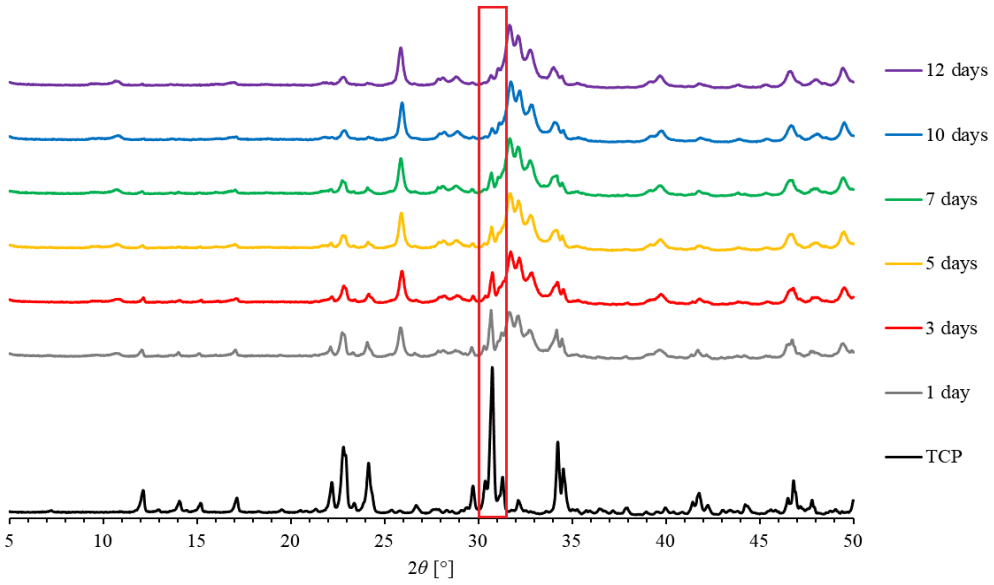

Figure 20: Comparison of diffractograms for CS0 samples, red square marks the main peak 30.74°

The first set of CS0 samples were left to set for 12 days to test the conversion of α-TCP to CDHA and establish an optimal setting time for samples. Diffractograms from the measurement are shown in Figure 20 where α-TCP as external standard has the highest intensity for 2θ angle 30.74°. The decrease in intensity of that peak, together with an increase in the intensity of other peaks, marks the conversion of α-TCP to CDHA. The conversion was calculated from the differences in intensity values of peak 30.74° and is shown in Figure 21 where after only one day the conversion is around 75 % and almost 90 % after 12 days. The initial CDHA conversion is important for its possible medical applications and is highly dependent on the quality and dryness of the prepared α-TCP. After 10 days, the conversion was sufficiently high and thus this setting time was chosen for further mechanical tests.

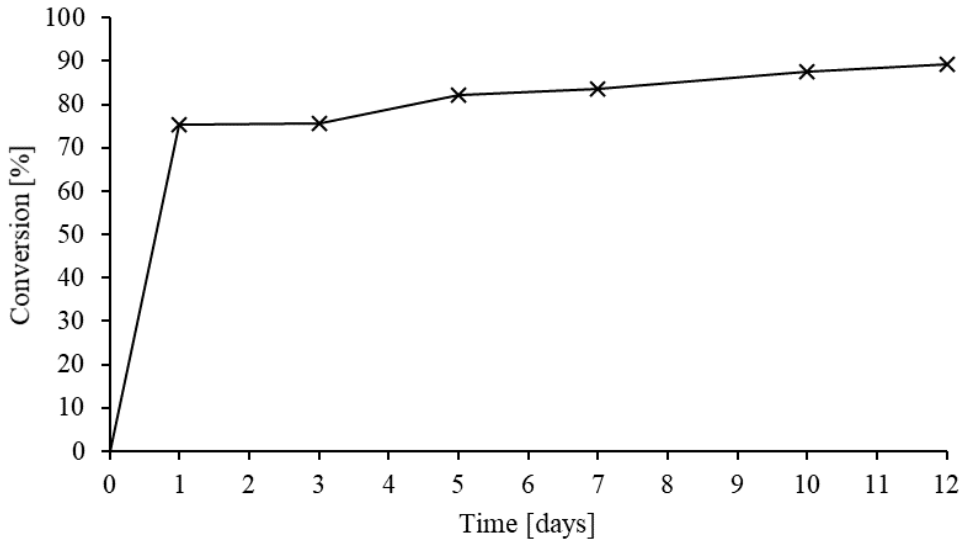

Figure 21: Conversion of α-TCP to CDHA in the first set of CS0 samples

The second set of CS0, CS0.5, CS1 and CS2 samples were measured to evaluate chitosan effect on the initial conversion. Figure 22 shows that CS0.5 have almost the same conversion as a control sample but the early conversion may be slightly affected for CS1 and CS2 which would indicate that chitosan slows the initial nucleation of CDHA crystals, however, after three days, the conversion is nearly the same for all samples and thereby chitosan does not affect the conversion in a long term. The small differences between conversion can be considered as deviation as the cement does not always set with the same conversion which can be caused by uneven cement distribution in the sample forms and also their slightly different dimensions.

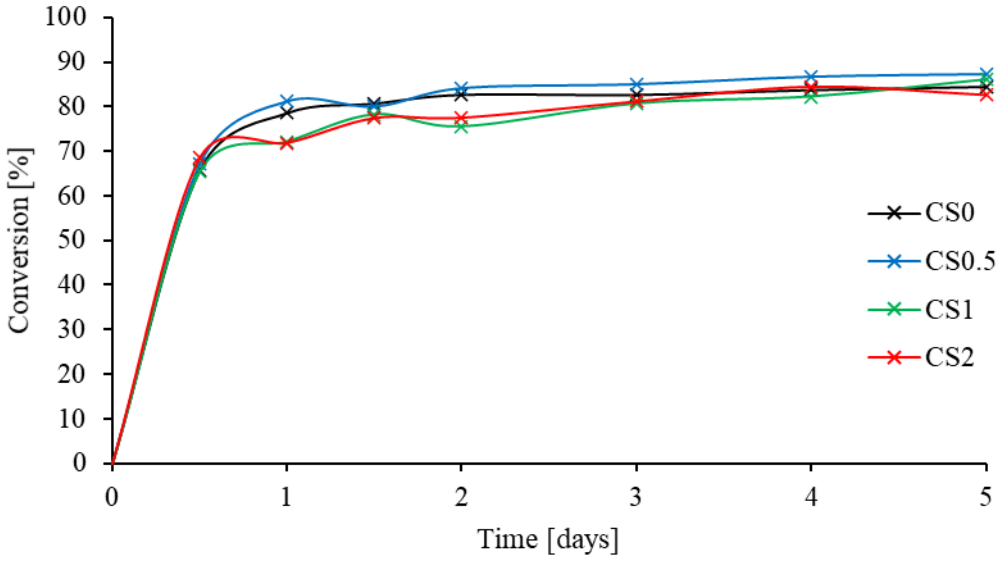

Figure 22: Conversion of α-TCP to CDHA for samples with different chitosan concentrations

5.4 Mechanical Testing

5.4.1 Cylindrical Calcium Phosphate Cement Samples

Tests under compression were performed with seven samples for each set of concentrations. All results are listed in Table 4 where some values have been discarded using Q-test or due to their non-linear and poor course during measurement which was probably caused by the creation of pores and uneven distribution in the cement during sample preparation. Equation 5 was used to calculate the compressive strength:

$$\sigma = \frac{F}{A} \tag{5}$$

Where σ is stress i.e. compressive strength (MPa), F is the standard force (N), and A is the base area of the individual specimen (mm^2). The highest improvement of compressive strength was observed for CS0.5 samples (23.97 ± 5.51 MPa) and slightly for CS1 samples (20.88 ± 2.76 MPa) compared to control samples CS0 (20.61 ± 5.20 MPa). Further increase of chitosan concentration leads to a decrease in compressive strength (19.04 ± 2.41 MPa for CS2). All values are compared in a bar graph shown in Figure 23 and stress-strain curves for each sample are shown in Figure 25. A similar trend was observed in the study with phosphorylated

chitosan by Wang et al. where mechanical properties also declined with increasing chitosan concentration [48]. However, T-test done in Excel showed that compared to control CS0 samples, the standard significance level of tested chitosan samples is higher than 0.05, therefore, no statistically significant increase or decrease in compressive strength was measured. Young's moduli were determined from the slope of the line of the curve's most linear part and comparison is shown in Figure 24. A small increase can be again observed for CS0.5 samples and decrease for samples with higher chitosan concentration. However, the goal was to determine the compressive strength and the measurement was not meant and optimized for evaluation of Young's modulus, therefore, these values are considered only approximate.

Table 4: Results from compressive strength testing

Sample No.	CS0		CS0.5		CS1		CS2	
	σ [MPa]	E [GPa]	σ [MPa]	E [GPa]	σ [MPa]	E [GPa]	σ [MPa]	E [GPa]
1	26.86	2.93	25.61	1.94	21.39	2.27	20.83	2.26
2	10.95	1.32	18.44	1.52	23.64	2.22	17.73	1.43
3	20.13	2.40	31.88	2.67	22.91	2.08	19.13	1.50
4	18.78	1.67	22.66	1.64	16.24	2.17	22.86	1.87
5	23.09	1.84	25.61	3.03	22.00	1.70	19.46	2.14
6	24.95	2.06	27.82	1.88	~~5.99~~	-	17.94	1.82
7	19.51	1.91	15.79	1.68	19.08	1.40	15.31	1.19
Average	**20.61**	**2.02**	**23.97**	**2.05**	**20.88**	**1.97**	**19.04**	**1.74**
Standard dev.	5.20	0.52	5.51	0.57	2.76	0.35	2.41	0.39

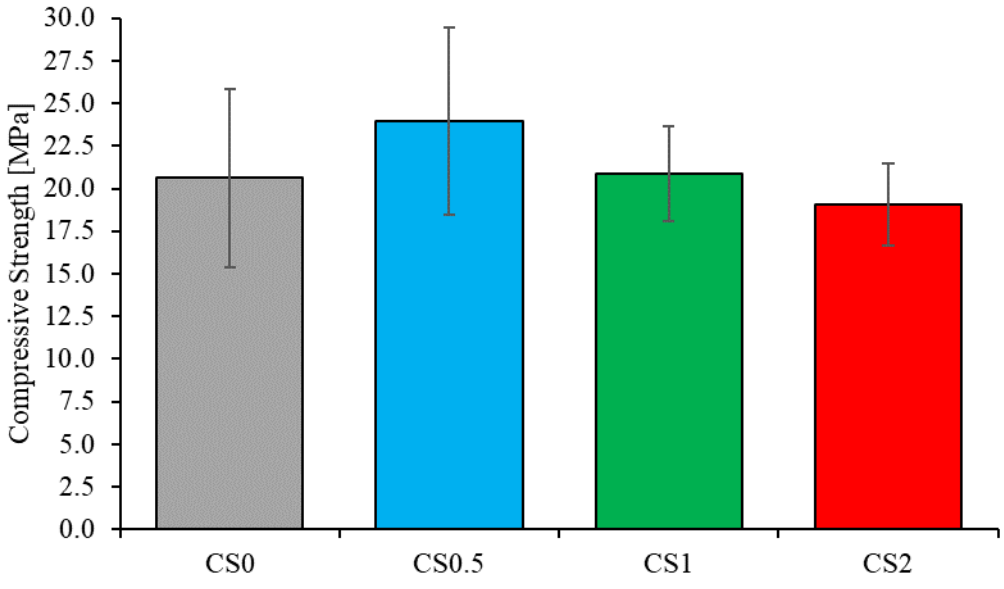

Figure 23: Bar graph comparison of compressive strengths of all samples

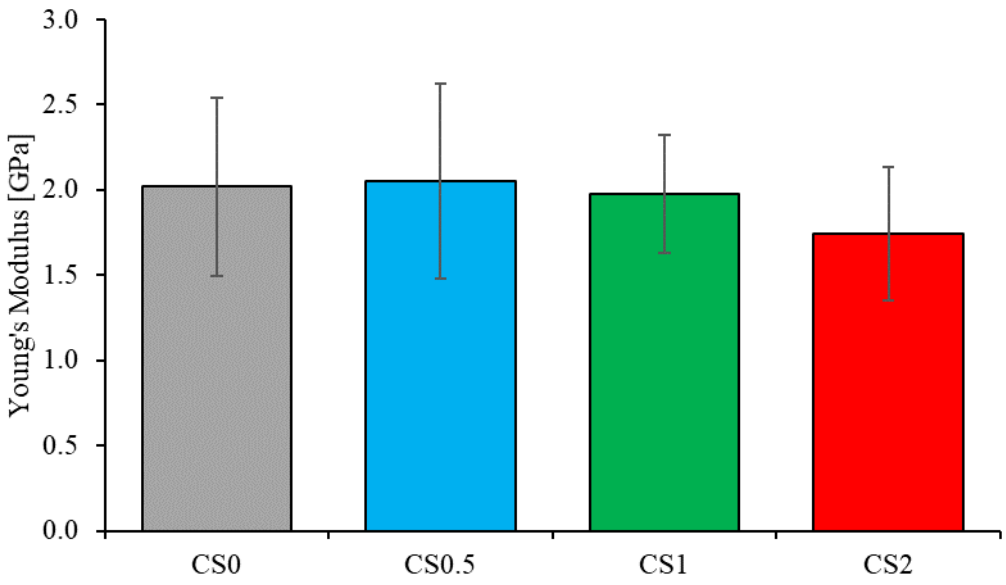

Figure 24: Bar graph comparison of Young's moduli

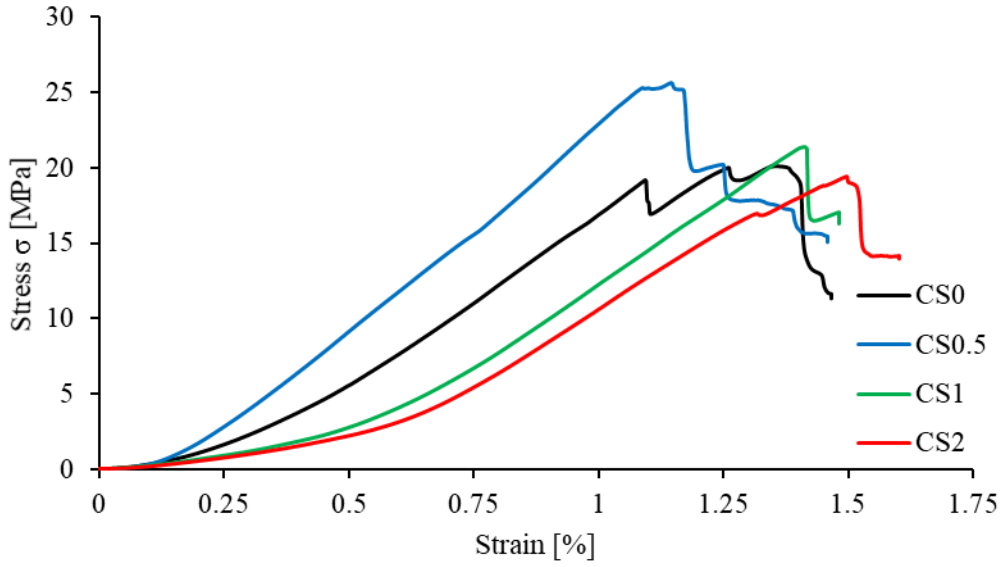

Figure 25: Comparison of most representative stress-strain curves

5.4.2 Adhesion Testing on Bone Samples

The most promising candidates for increased adhesion e.g. CS0.5 and CS1 as well as control sample CS0 were used in actual bone specimen tests. Due to the advanced nature of the adhesion test and limited availability of bones only three bone specimens were tested. Glued bones were taken out from the water bath after one day and used for measurement without any further adjustments (Figure 26). Unfortunately, CS0.5 and CS1 bone samples shifted and slightly slid down during the preparation and incubation which may have a negative effect on the results. CS0 sample was joined almost perfectly without any shifting.

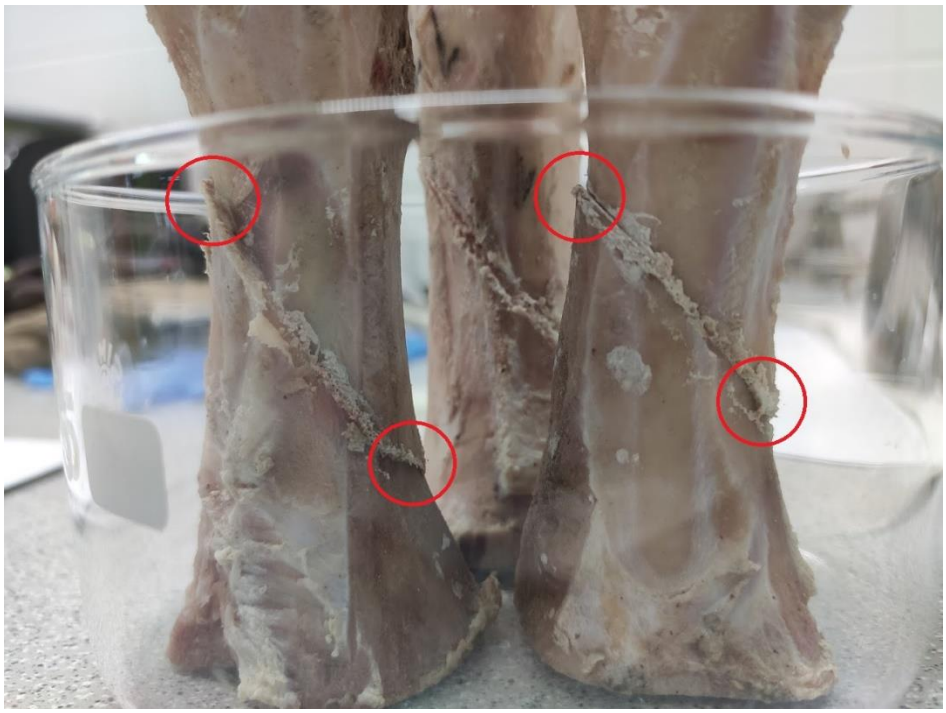

Figure 26: Glued bones after one day of incubation, left: CS0.5, middle: CS0, right: CS1. Red circles mark the shifts of bones which occurred during preparation and incubation

Similar to the cylindrical specimens, equation 6 was used to calculate the compressive strength τ:

$$\tau = \frac{F \cdot \cos 45°}{A} \tag{6}$$

where F is the standard force (N), and A is the base area of the individual specimen (mm^2) and 45° is the angle of the cut. Figure 27 shows the results of compressive tests. Highest compressive strength was measured for CS0 sample, whereas CS0.5 sample had significantly lower compressive strength. CS1 sample achieved higher compressive strength than CS0.5 but still lower than the CS0 sample. Compressive strengths of all bone samples are compared in a bar graph in Figure 28. Chitosan samples were expected to exhibit higher compressive strength than the CS0 sample as when the cement alone was tested. Some increase can be considered between CS0.5 and CS1 samples as both samples shifted during preparation.

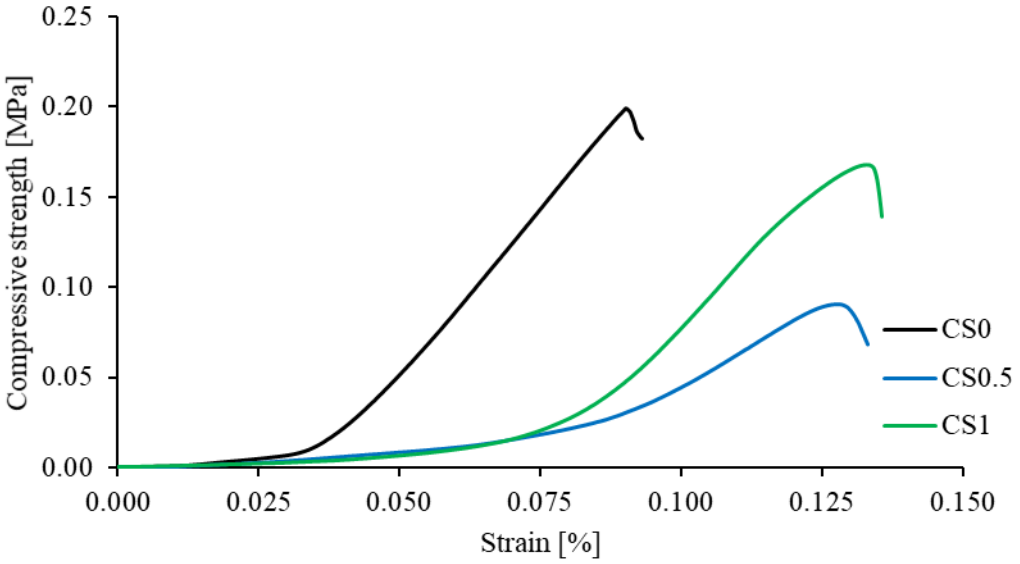

Figure 27: Stress-strain diagram of glued bone samples

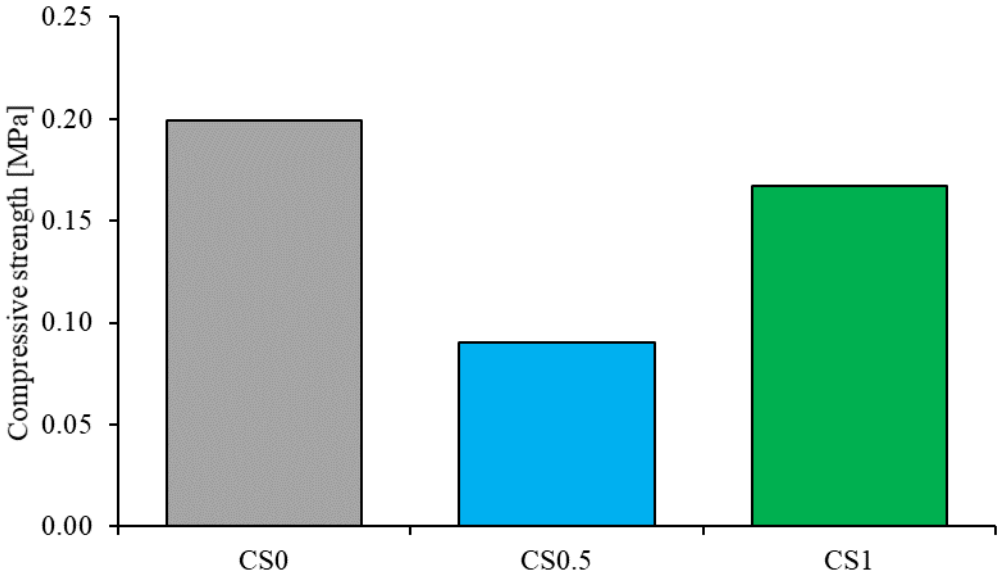

Figure 28: Bar graph comparison of the highest compressive strengths of bone samples

On the other hand, chitosan samples withstood a higher strain before they fractured compared to the control sample as shown in a bar graph in Figure 29. This implies that chitosan samples may have a lower overall compressive strength but can withstand a higher strain and thus they have higher elasticity. All cross-sections after the compressive tests are shown in Figure 30 where every sample have almost the same fracture interface. Certain adhesion can be observed as only half of the cement is torn down from the bone surface but nonetheless, it was not strong enough as expected. However, these unexpected results can be attributed to the fact that each bone had slightly different anatomy and cross-section surface area. Together with the already mentioned shifts during preparation, this measurement is complicated and difficult to reproduce as the preparation and sawing of the bones to prepare equal samples is also more difficult than expected. For all these reasons this measurement is thus considered as

inconclusive and further research into the topic is required to provide better results. Some recommendations for further possible tests using bone samples are presented in chapter 6.

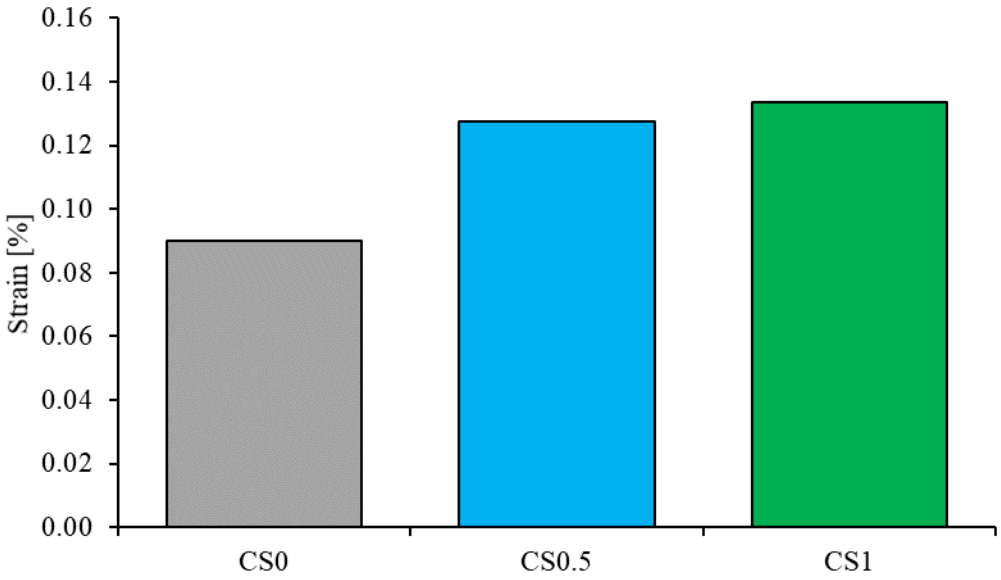

Figure 29: Bar graph comparison of strain applied to bone samples

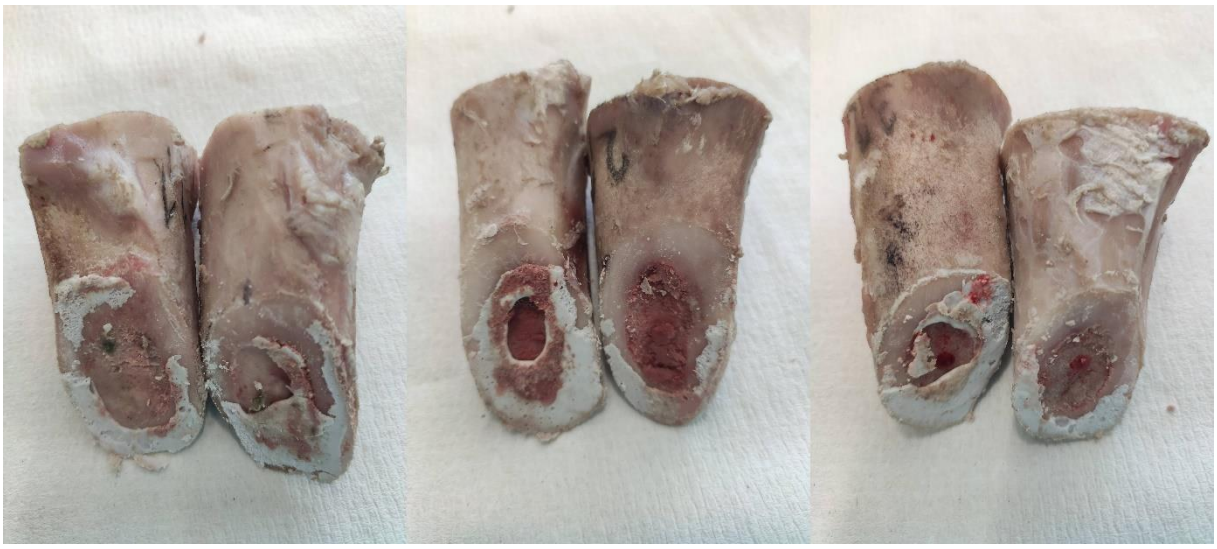

Figure 30: Bone cross-sections after the compressive test, from left to right: CS0, CS0.5 and CS1

6 CONCLUSION

The aim of this work was to evaluate the chitosan effect on the properties of calcium phosphate cement. This work dealt with the preparation of calcium phosphate cements with chitosan and their characterization using static mechanical tests, X-ray diffraction and rheology. In the theoretical part, literary research on polymeric additives to CPCs was written.

Rheology was initially intended to measure adhesiveness of the copolymer solution with chitosan. However, due to the inhomogeneity of chitosan samples, it was not possible to reproduce measurements with desirable certainty. Two different methods of preparation were tested using magnetic stirrer and centrifugation, but neither one was effective enough to eliminate this problem. It is necessary to optimize the preparation method of copolymer solution and some recommendations for further research are proposed here. Though centrifugation proved as a viable preparation method, some adjustments must be made in order to prepare more homogeneous solutions. The first possibility is to prepare copolymer and chitosan solutions separately and mix them after they are both sufficiently dissolved. For better solubility, the chitosan could be milled to obtain smaller particles. Dissolving chitosan below the gelation temperature of PLGA-PEG-PLGA copolymer at temperature for example 20 – 30 °C could also help the dissolution. The use of substituted chitosan with better solubility or chitosan with lower molecular weight should also be considered. Moreover, adding chitosan into the powder phase would also help, however, liquid to powder ratio (L/P) would have been changed as well in order to keep optimal viscosity and injectability of the paste. Nevertheless, via this procedure, higher amount of chitosan would be possible to add.

Cement paste was also measured using rheology to evaluate flow properties after the addition of chitosan. It was found out that low chitosan concentrations (CS0.5) improve the flow properties and slightly slow the setting at 23 °C and also at 37 °C. At 37 °C, the CS2 sample setting time is almost similar to control CS0 sample but CS1 samples set faster compared to the others. All cement pastes samples were easily injectable through the syringe.

XRD measurements were performed with different sets of samples to find out if chitosan affects the conversion of α-TCP to CDHA. The results showed that chitosan might affect the initial conversion in higher concentrations but does not affect it in the long term because, after three days, the conversion was almost the same for all samples and differences were neglectable.

Static mechanical tests were performed on cylindrical cement specimens to determine chitosan effect on the compressive strength of the cement. It was found out that chitosan slightly improves the compressive strength but only in lower concentrations. CS0.5 samples showed the highest compressive strength (23.97 ± 5.51 MPa) compared to the control CS0 sample (20.61 ± 5.20 MPa). CS1 sample had almost the same compressive strength as the control sample (20.88 ± 2.76 MPa). With increasing chitosan concentration, the compressive strength declined for CS2 sample (19.04 ± 2.41 MPa). This difference in compressive strengths between control and chitosan samples is not statistically significant, however, samples with higher chitosan concentration were more inhomogeneous and higher amount of chitosan interacted with water which is needed for the conversion of α-TCP to CDHA as the reaction is hydrolytic. Moreover, an increased amount of chitosan may suppress CDHA crystallization in terms of the

crystal size thus affecting the cement strength. On the other hand, samples with lower chitosan concentration were more homogeneous and with the lower amount of chitosan there, was more water available for the conversion and crystals can grow and hook up more closely and tighter.

The last measurement was to evaluate the adhesion strength of the cement when applied to bone samples. The measurement was performed by static pressure tests to measure compressive strength. Results showed that the highest compressive strength was measured for control CS0 sample compared to chitosan samples which had lower compressive strength, however, they withstood a higher strain indicating a better elasticity. The lower compressive strength was attributed to the fact that chitosan bone samples shifted during preparation and were not joined perfectly. Also, slightly different anatomy of each bone presented a complication. For these reasons, this measurement was considered as inconclusive. For further measurements, more bone samples are required and also the use of splint could eliminate any shifts and improve the sample preparation. Also, instead of using large porcine femur, rabbit femur bone could be used for better manipulation and more precise samples. Furthermore, the use of epoxy resin would help in the preparation of better parallel contact surfaces. On the other hand, testing the adhesion of bioceramic materials is not a standard method and although this experiment failed, important knowledge has been gained about what to avoid and what to improve.

7 REFERENCES

[1] GINEBRA, Maria-Pau, Cristina CANAL, Montserrat ESPANOL, David PASTORINO and Edgar B. MONTUFAR. Calcium phosphate cements as drug delivery materials. *Advanced Drug Delivery Reviews*. 2012, **64**(12), 1090-1110. DOI: 10.1016/j.addr.2012.01.008. ISSN 0169409X. Available from: https://linkinghub.elsevier.com/retrieve/pii/S0169409X12000117

[2] YOUSEFI, Azizeh-Mitra. A review of calcium phosphate cements and acrylic bone cements as injectable materials for bone repair and implant fixation. *Journal of Applied Biomaterials & Functional Materials*. 2019, **17**(4), 1-21. DOI: 10.1177/2280800019872594. ISSN 2280-8000. Available from: http://journals.sagepub.com/doi/10.1177/2280800019872594

[3] CLARKE, Bart. Normal Bone Anatomy and Physiology. *Clinical Journal of the American Society of Nephrology*. 2008, **3**(Supplement 3), S131-S139. DOI: 10.2215/CJN.04151206. ISSN 1555-9041. Available from: http://cjasn.asnjournals.org/lookup/doi/10.2215/CJN.04151206

[4] DOROZHKIN, S.V. and M. EPPLE. Biological and Medical Significance of Calcium Phosphates. Angewandte *Chemie International*. 2002, **41**(17), 3130-3146. DOI: 10.1002/1521-3773(20020902)41:17<3130::AID-ANIE3130>3.0.CO;2-1.

[5] Internal structure of a human long bone. In: *Encyclopædia Britannica* [online]. Encyclopædia Britannica, 2019 [cit. 2020-03-01]. Available from: https://www.britannica.com/science/bone-anatomy/Bone-morphology#/media/1/72869/66017

[6] CAMPAGNE, Danielle. Overview of Fractures. *MSD Manuals* [online]. Kenilworth (USA): Merck Sharp & Dohme Corp., a subsidiary of Merck & Cp., c2020 [cit. 2020-04-18]. Available from: https://www.msdmanuals.com/en-gb/home/injuries-and-poisoning/fractures/overview-of-fractures

[7] Osteoporosis Overview. *NIH Osteoporosis and Related Bone Diseases National Resource Center* [online]. Bethesda (MD): National Institutes of Health, 2018 [cit. 2020-04-18]. Available from: https://www.bones.nih.gov/health-info/bone/osteoporosis/overview#Prevention

[8] SUHM, Norbert and Armando GISEP. Injectable Bone Cement Augmentation for the Treatment of Distal Radius Fractures: A Review. *Journal of Orthopaedic Trauma*. 2008, **22**, S121-S125. DOI: 10.1097/BOT.0b013e3181830d13. ISSN 0890-5339. Available from: http://journals.lww.com/00005131-200809008-00011

[9] GINEBRA, Maria-Pau and Edgar B. MONTUFAR. Cements as bone repair materials. *Bone Repair Biomaterials*. Elsevier, 2019, 2019, 233-271. DOI: 10.1016/B978-0-08-102451-5.00009-3. ISBN 9780081024515. Available from: https://linkinghub.elsevier.com/retrieve/pii/B9780081024515000093

[10] LEWIS, Gladius. Viscoelastic properties of injectable bone cements for orthopaedic applications: State-of-the-art review. *Journal of Biomedical Materials Research Part B: Applied Biomaterials*. 2011, **98B**(1), 171-191. DOI: 10.1002/jbm.b.31835. ISSN 15524973. Available from: http://doi.wiley.com/10.1002/jbm.b.31835

[11] MAGNAN, B., M. BONDI, T. MALUTA, E. SAMAILA, L. SCHIRRU and C. DALL'OCA. Acrylic bone cement: current concept review. *MUSCULOSKELETAL SURGERY*. 2013, **97**(2), 93-100. DOI: 10.1007/s12306-013-0293-9. ISSN 2035-5106. Available from: http://link.springer.com/10.1007/s12306-013-0293-9

[12] KUCKO, Nathan W., Ralf-Peter HERBER, Sander C.G. LEEUWENBURGH and John A. JANSEN. Calcium Phosphate Bioceramics and Cements. *Principles of Regenerative Medicine*. Elsevier, 2019, 2019, , 591-611. DOI: 10.1016/B978-0-12-809880-6.00034-5. ISBN 9780128098806. Available from: https://linkinghub.elsevier.com/retrieve/pii/B9780128098806000345

[13] SPIVAK, Jeffrey. Vertebroplasty and Kyphoplasty Comparisons. SPINE-health [online]. Deerfield (IL): Veritas Health, c1999-2020 [cit. 2020-05-04]. Available from: https://www.spine-health.com/treatment/back-surgery/vertebroplasty-and-kyphoplasty-comparisons

[14] DOROZHKIN, Sergey. Self-Setting Calcium Orthophosphate Formulations. *Journal of Functional Biomaterials*. 2013, **4**(4), 209-311. DOI: 10.3390/jfb4040209. ISSN 2079-4983. Available from: http://www.mdpi.com/2079-4983/4/4/209

[15] M., Bohner. Physical and chemical aspects of calcium phosphates used in spinal surgery. *European* Spine *Journal*. 2001, **10**, S114-S121. DOI: 10.1007/s005860100276. ISSN 0940-6719. Available from: http://link.springer.com/10.1007/s005860100276

[16] DOROZHKIN, Sergey. Calcium Orthophosphates in Nature, Biology and Medicine. *Materials*. 2009, **2**(2), 399-498. DOI: 10.3390/ma2020399. ISSN 1996-1944. Available from: http://www.mdpi.com/1996-1944/2/2/399

[17] CARRODEGUAS, R.G. and S. DE AZA. α-Tricalcium phosphate: Synthesis, properties and biomedical applications. *Acta Biomaterialia*. 2011, **7**(10), 3536-3546. DOI: 10.1016/j.actbio.2011.06.019. ISSN 17427061. Available from: https://linkinghub.elsevier.com/retrieve/pii/S174270611100256X

[18] BOHNER, M., U. GBURECK and J.E. BARRALET. Technological issues for the development of more efficient calcium phosphate bone cements: A critical assessment. *Biomaterials*. 2005, **26**(33), 6423-6429. DOI: 10.1016/j.biomaterials.2005.03.049. ISSN 01429612. Available from: https://linkinghub.elsevier.com/retrieve/pii/S0142961205003844

[19] MAAZOUZ, Yassine, Edgar B. MONTUFAR, Julien MALBERT, Montserrat ESPANOL and Maria-Pau GINEBRA. Self-hardening and thermoresponsive alpha tricalcium phosphate/pluronic pastes. *Acta Biomaterialia*. 2017, **49**, 563-574. DOI: 10.1016/j.actbio.2016.11.043. ISSN 17427061. Available from: https://linkinghub.elsevier.com/retrieve/pii/S1742706116306407

[20] QIAO, Mingxi, Dawei CHEN, Xichen MA and Yanjun LIU. Injectable biodegradable temperature-responsive PLGA–PEG–PLGA copolymers: Synthesis and effect of copolymer composition on the drug release from the copolymer-based hydrogels. *International Journal of Pharmaceutics*. 2005, **294**(1-2), 103-112. DOI: 10.1016/j.ijpharm.2005.01.017. ISSN 03785173. Available from: https://linkinghub.elsevier.com/retrieve/pii/S0378517305000840

[21] VOJTOVA, Lucy, Lenka MICHLOVSKA, Kristyna VALOVA, et al. The Effect of the Thermosensitive Biodegradable PLGA–PEG–PLGA Copolymer on the Rheological, Structural and Mechanical Properties of Thixotropic Self-Hardening Tricalcium Phosphate Cement. *International Journal of Molecular Sciences*. 2019, **20**(2). DOI: 10.3390/ijms20020391. ISSN 1422-0067. Available from: http://www.mdpi.com/1422-0067/20/2/391

[22] BIGI, A., P. TORRICELLI, M. FINI, B. BRACCI, S. PANZAVOLTA, L. STURBA and R. GIARDINO. A Biomimetic Gelatin-Calcium Phosphate Bone Cement. *The International Journal of Artificial Organs*. 2018, **27**(8), 664-673. DOI: 10.1177/039139880402700804. ISSN 0391-3988. Available from: http://journals.sagepub.com/doi/10.1177/039139880402700804

[23] BIGI, A., B. BRACCI and S. PANZAVOLTA. Effect of added gelatin on the properties of calcium phosphate cement. *Biomaterials*. 2004, **25**(14), 2893-2899. DOI: 10.1016/j.biomaterials.2003.09.059. ISSN 01429612. Available from: https://linkinghub.elsevier.com/retrieve/pii/S0142961203008019

[24] PANZAVOLTA, S., P. TORRICELLI, L. STURBA, B. BRACCI, R. GIARDINO and A. BIGI. Setting properties and in vitro bioactivity of strontium-enriched gelatin–calcium phosphate bone cements. *Journal of Biomedical Materials Research Part A*. 2008, **84A**(4), 965-972. DOI: 10.1002/jbm.a.31412. ISSN 15493296. Available from: http://doi.wiley.com/10.1002/jbm.a.31412

[25] LOPEZ-HEREDIA, M. A., J. PATTIPEILOHY, S. HSU, et al. Bulk physicochemical, interconnectivity, and mechanical properties of calcium phosphate cements-fibrin glue composites for bone substitute applications. *Journal of Biomedical Materials Research Part A*. 2013, **101A**(2), 478-490. DOI: 10.1002/jbm.a.34342. ISSN 15493296. Available from: http://doi.wiley.com/10.1002/jbm.a.34342

[26] CUI, Geng, Jie LI, Wei LEI, Long BI, Peifu TANG, Yutian LIANG, Sheng TAO and Yan WANG. The mechanical and biological properties of an injectable calcium phosphate cement-fibrin glue composite for bone regeneration. *Journal of Biomedical Materials Research Part B: Applied Biomaterials*. 2009, **92B**(2), 377-385. DOI: 10.1002/jbm.b.31525. ISSN 15524973. Available from: http://doi.wiley.com/10.1002/jbm.b.31525

[27] PEREZ, Roman A, Hae-Won KIM and Maria-Pau GINEBRA. Polymeric additives to enhance the functional properties of calcium phosphate cements. *Journal of Tissue Engineering*. 2012, **3**(1). DOI: 10.1177/2041731412439555. ISSN 2041-7314. Available from: http://journals.sagepub.com/doi/10.1177/2041731412439555

[28] LEE, Gil-Su, Jeong-Hui PARK, Jong-Eun WON, Ueon Sang SHIN and Hae-Won KIM. Alginate combined calcium phosphate cements: mechanical properties and in vitro rat bone marrow stromal cell responses. *Journal of Materials Science: Materials in Medicine*. 2011, **22**(5), 1257-1268. DOI: 10.1007/s10856-011-4296-5. ISSN 0957-4530. Available from: http://link.springer.com/10.1007/s10856-011-4296-5

[29] QI, Xiaopeng, Jiandong YE and Yingjun WANG. Alginate/poly (lactic- co -glycolic acid)/calcium phosphate cement scaffold with oriented pore structure for bone tissue engineering. *Journal of Biomedical Materials Research Part A*. 2009, **89A**(4), 980-987. DOI: 10.1002/jbm.a.32054. ISSN 15493296. Available from: http://doi.wiley.com/10.1002/jbm.a.32054

[30] LIU, Zongguang, Shuxin QU, Xiaotong ZHENG, Xiong XIONG, Rong FU, Kuangyun TANG, Zhendong ZHONG and Jie WENG. Effect of polydopamine on the biomimetic mineralization of mussel-inspired calcium phosphate cement in vitro. *Materials Science and Engineering: C*. 2014, **44**, 44-51. DOI: 10.1016/j.msec.2014.07.063. ISSN 09284931. Available from: https://linkinghub.elsevier.com/retrieve/pii/S0928493114004810

[31] LIU, Zongguang, Jianmei CHEN, Guowei ZHANG, et al. Enhanced Repairing of Critical-Sized Calvarial Bone Defects by Mussel-Inspired Calcium Phosphate Cement. *ACS Biomaterials Science & Engineering*. 2018, **4**(5), 1852-1861. DOI: 10.1021/acsbiomaterials.8b00243. ISSN 2373-9878. Available from: https://pubs.acs.org/doi/10.1021/acsbiomaterials.8b00243

[32] BERCIER, Ariane, Stéphane GONÇALVES, Olivier LIGNON and Juliette FITREMANN. Calcium Phosphate Bone Cements Including Sugar Surfactants: Part One—Porosity, Setting Times and Compressive Strength. *Materials*. 2010, **3**(10), 4695-4709. DOI: 10.3390/ma3104695. ISSN 1996-1944. Available from: http://www.mdpi.com/1996-1944/3/10/4695

[33] BERCIER, Ariane, Stéphane GONÇALVES, Helène AUTEFAGE, Fabienne BRIAND-MESANGE, Olivier LIGNON and Juliette FITREMANN. Calcium Phosphate Bone Cements Including Sugar Surfactants: Part Two—Injectability, Adhesive Properties and Biocompatibility. *Materials*. 2010, **3**(12), 5111-5129. DOI: 10.3390/ma3125111. ISSN 1996-1944. Available from: http://www.mdpi.com/1996-1944/3/12/5111

[34] RINAUDO, Marguerite. Chitin and chitosan: Properties and applications. *Progress in Polymer Science*. 2006, **31**(7), 603-632. DOI: 10.1016/j.progpolymsci.2006.06.001. ISSN 00796700. Available from: https://linkinghub.elsevier.com/retrieve/pii/S0079670006000530

[35] MATI-BAOUCHE, Narimane, Pierre-Henri ELCHINGER, Hélène DE BAYNAST, Guillaume PIERRE, Cédric DELATTRE and Philippe MICHAUD. Chitosan as an adhesive. *European Polymer Journal*. 2014, **60**, 198-212. DOI: 10.1016/j.eurpolymj.2014.09.008. ISSN 00143057. Available from: https://linkinghub.elsevier.com/retrieve/pii/S0014305714003267

[36] ARANAZ, Inmaculada, Marian MENGIBAR, Ruth HARRIS, Ines PANOS, Beatriz MIRALLES, Niuris ACOSTA, Gemma GALED and Angeles HERAS. Functional Characterization of Chitin and Chitosan. *Current Chemical Biology*. 2009, **3**(2), 203-230. DOI: 10.2174/187231309788166415. ISSN 18723136.

[37] RINAUDO, M., F. CHIELLINI, R.M. OTTENBRITE and E. CHIELLINI. Chitosan—A versatile semi-synthetic polymer in biomedical applications: Properties and applications. *Progress in Polymer Science*. 2011, **36**(8), 981-1014. DOI: 10.1016/j.progpolymsci.2011.02.001. ISSN 00796700. Available from: https://linkinghub.elsevier.com/retrieve/pii/S007967001100027X

[38] CHENITE, A, C CHAPUT, D WANG, et al. Novel injectable neutral solutions of chitosan form biodegradable gels in situ. *Biomaterials*. 2000, **21**(21), 2155-2161. DOI: 10.1016/S0142-9612(00)00116-2. ISSN 01429612. Available from: https://linkinghub.elsevier.com/retrieve/pii/S0142961200001162

[39] KEAN, T. and M. THANOU. Biodegradation, biodistribution and toxicity of chitosan. *Advanced Drug Delivery Reviews*. 2010, **62**(1), 3-11. DOI: 10.1016/j.addr.2009.09.004. ISSN 0169409X. Available from: https://linkinghub.elsevier.com/retrieve/pii/S0169409X0900283X

[40] CHATELET, C. Influence of the degree of acetylation on some biological properties of chitosan films. *Biomaterials*. **22**(3), 261-268. DOI: 10.1016/S0142-9612(00)00183-6. ISSN 01429612. Available from: https://linkinghub.elsevier.com/retrieve/pii/S0142961200001836

[41] FUNKHOUSER, Jane D and Nathan N ARONSON. Chitinase family GH18: evolutionary insights from the genomic history of a diverse protein family. *BMC Evolutionary Biology*. 2007, **7**(1). DOI: 10.1186/1471-2148-7-96. ISSN 1471-2148. Available from: https://bmcevolbiol.biomedcentral.com/articles/10.1186/1471-2148-7-96

[42] OKAMOTO, Y. Analgesic effects of chitin and chitosan. *Carbohydrate Polymers*. **49**(3), 249-252. DOI: 10.1016/S0144-8617(01)00316-2. ISSN 01448617. Available from: https://linkinghub.elsevier.com/retrieve/pii/S0144861701003162

[43] KHANLARI, Samaneh and Marc A. DUBÉ. Bioadhesives: A Review. *Macromolecular Reaction Engineering*. 2013, **7**(11), 573-587. DOI: 10.1002/mren.201300114. ISSN 1862832X. Available from: http://doi.wiley.com/10.1002/mren.201300114

[44] BURKATOVSKAYA, Marina, George P TEGOS, Emilia SWIETLIK, Tatiana N DEMIDOVA, Ana P CASTANO and Michael R. HAMBLIN. Use of chitosan bandage to prevent fatal infections developing from highly contaminated wounds in mice. *Biomaterials*. 2006, **27**(22), 4157-4164. DOI: 10.1016/j.biomaterials.2006.03.028. ISSN 01429612. Available from: https://linkinghub.elsevier.com/retrieve/pii/S0142961206002614

[45] BERGER, J., M. REIST, J.M. MAYER, O. FELT, N.A. PEPPAS and R. GURNY. Structure and interactions in covalently and ionically crosslinked chitosan hydrogels for biomedical applications. *European Journal of Pharmaceutics and Biopharmaceutics*. 2004, **57**(1), 19-34. DOI: 10.1016/S0939-6411(03)00161-9. ISSN 09396411. Available from: https://linkinghub.elsevier.com/retrieve/pii/S0939641103001619

[46] YOKOYAMA, Atsuro, Satoru YAMAMOTO, Takao KAWASAKI, Takao KOHGO and Masanori NAKASU. Development of calcium phosphate cement using chitosan and citric acid for bone substitute materials. Biomaterials. 2002, **23**(4), 1091-1101. DOI: 10.1016/S0142-9612(01)00221-6. ISSN 01429612. Available from: https://linkinghub.elsevier.com/retrieve/pii/S0142961201002216

[47] TAKECHI, Masaaki, Youji MIYAMOTO, Kunio ISHIKAWA, Taketomo TOH, Tetsuya YUASA, Masarus NAGAYAMA and Kazuomi SUZUKI. Initial histological evaluation of anti-washout type fast-setting calcium phosphate cement following subcutaneous implantation. *Biomaterials*. 1998, **19**(22), 2057-2063. DOI: 10.1016/S0142-9612(98)00114-8. ISSN 01429612. Available from: https://linkinghub.elsevier.com/retrieve/pii/S0142961298001148

[48] WANG, Xiaohong, Jianbiao MA, Yinong WANG and Binglin HE. Structural characterization of phosphorylated chitosan and their applications as effective additives of calcium phosphate cements. *Biomaterials*. 2001, **22**(16), 2247-2255. DOI: 10.1016/S0142-9612(00)00413-0. ISSN 01429612. Available from: https://linkinghub.elsevier.com/retrieve/pii/S0142961200004130

[49] SUN, Limin, Hockin H. K. XU, Shozo TAKAGI and Laurence C. CHOW. Fast Setting Calcium Phosphate Cement-Chitosan Composite: Mechanical Properties and Dissolution Rates. *Journal of Biomaterials Applications*. 2006, **21**(3), 299-315. DOI: 10.1177/0885328206063687. ISSN 0885-3282. Available from: http://journals.sagepub.com/doi/10.1177/0885328206063687

[50] CHERNG, A., S. TAKAGI and L. C. CHOW. Effects of hydroxypropyl methylcellulose and other gelling agents on the handling properties of calcium phosphate cement. *Journal of Biomedical Materials Research*. 1997, **35**(3), 273-277. DOI: 10.1002/(SICI)1097-4636(19970605)35:3<273::AID-JBM1>3.0.CO;2-E.

[51] MICHLOVSKÁ, Lenka, Lucy VOJTOVÁ, Ludmila MRAVCOVÁ, Soňa HERMANOVÁ, Jiří KUČERÍK and Josef JANČÁŘ. Functionalization Conditions of PLGA-PEG-PLGA Copolymer with Itaconic Anhydride. *Macromolecular Symposia*. 2010, **295**(1), 119-124. DOI: 10.1002/masy.200900071. ISSN 10221360. Available from: http://doi.wiley.com/10.1002/masy.200900071

[52] MONTUFAR, E.B., Y. MAAZOUZ and M.P. GINEBRA. Relevance of the setting reaction to the injectability of tricalcium phosphate pastes. *Acta Biomaterialia*. 2013, **9**(4), 6188-6198. DOI: 10.1016/j.actbio.2012.11.028. ISSN 17427061. Available from: https://linkinghub.elsevier.com/retrieve/pii/S1742706112005788

[53] RAMACHADRAN, V.S and James J. BEAUDOIN. *Handbook of analytical techniques in concrete science and technology: principles, techniques and applications* [online]. Park Ridge, NJ: Noyes Publications, 2001 [cit. 2020-05-14]. ISBN 978-0-8155-1437-2. Available from: https://app.knovel.com/web/toc.v/cid:kpHATCST01/viewerType:toc/

[54] What is Compression Testing? *Instron* [online]. Norwood (MA): Illinois Tool Works, c2014 [cit. 2020-05-27]. Available from: https://www.instron.us/en-us/our-company/library/test-types/compression-test

[55] Young's modulus. *Encyclopædia Britannica* [online]. Chicago (IL): Encyclopædia Britannica, 2019 [cit. 2020-05-28]. Available from: https://www.britannica.com/science/Youngs-modulus

[56] Basics of rheology. *Anton Paar* [online]. Graz (Austria): Anton Paar, c2020 [cit. 2020-05-31]. Available from: https://wiki.anton-paar.com/en/basics-of-rheology/

[57] TA Instruments, 2018, Rheological Evaluation of Adhesives - TA Instruments Webinar Series, YouTube video. [2020-07-13]. Available from: https://www.youtube.com/watch?v=paoSBlXpYtQ

8 LIST OF ABBREVIATIONS

IBC	injectable bone cement
CPC	calcium phosphate cement
CSC	calcium sulfate cement
ABC	acrylic bone cement
BPO	benzoyl peroxide
DMT	*N*,*N*-dimethyl-*p*-toluidine
MMA	methyl methacrylate
PMMA	poly(methyl methacrylate)
CaP	calcium phosphate
MCPM	monocalcium phosphate monohydrate
MCPA	monocalcium phosphate anhydrous
DCPD	dicalcium phosphate dihydrate
DCPA	dicalcium phosphate anhydrous
TCP	tricalcium phosphate
TTCP	tetracalcium phosphate
OCP	octacalcium phosphate
ACP	amorphous calcium phosphate
HA	hydroxyapatite
PHA	precipitated hydroxyapatite
CDHA	calcium deficit hydroxyapatite
PEO	polyoxoethylene
PPO	polyoxopropylene
PLGA	poly(lactic-co-glycolic acid)
PEG	polyethylene glycol
DD	deacetylation degree
MW	molecular weight
HPN	hybrid polymer network
IPN	interpenetrating polymer network
XRD	X-ray diffraction
P-chitosan	phosphorylated chitosan
FG	fibrin glue
DOPA	3,4-dihydroxy-L-phenylalanine
PDA	polydopamine
SEM	scanning electron microscope
CS	chitosan
PET	polyethylene terephthalate
LVE	linear viscoelastic region

9 LIST OF FIGURES

10 LIST OF TABLES